Anderson Ricardo Ingracio

A BUSCA DE MEDIADORES PARA A MODULAÇÃO DE COLÁGENO: EFEITO DE MOLÉCULAS ATIVAS INCORPORADAS A BIOMATERIAL POLIMÉRICO

Dissertação apresentada à Universidade de Caxias do Sul, como pré-requisito para obtenção do Título de Mestre em Ciências da Saúde.

Caxias do Sul

2018

Anderson Ricardo Ingracio

A BUSCA DE MEDIADORES PARA A MODULAÇÃO DE COLÁGENO: EFEITO DE MOLÉCULAS ATIVAS INCORPORADAS A BIOMATERIAL POLIMÉRICO

Dissertação apresentada à Universidade de Caxias do Sul, como pré-requisito para obtenção do Título de Mestre em Ciências da Saúde.

Orientador: Prof. Dr. Asdrubal Falavigna
Co-Orientador: Prof. Dr. Otávio Bianchi

Caxias do Sul

2018

Dados Internacionais de Catalogação na Publicação (CIP)
Universidade de Caxias do Sul
UCS - BICE - Processamento Técnico

I54b Ingracio, Anderson Ricardo, 1977-
A busca de mediadores para a modulação de colágeno : efeito de moléculas ativas incorporadas a biomaterial polimérico / Anderson Ricardo Ingracio. – 2018.
vii, 58 f. : il. ; 30 cm

Apresenta bibliografia.
Dissertação (Mestrado) – Universidade de Caxias do Sul, Programa de Pós-Graduação em Ciências da Saúde, 2018.
Orientação: Prof. Dr. Asdrubal Falavigna.
Coorientação: Prof. Dr. Otávio Bianchi.

1. Colágeno. 2. Sangue - Lipoproteínas. 3. Cicatrização de ferimentos. I. Falavigna, Asdrubal, orient. II. Bianchi, Otávio, coorient. III. Título.

CDU 2. ed.: 547.962.9

Índice para o catálogo sistemático:

1. Colágeno	547.962.9
2. Sangue - Lipoproteínas	612.11:577.112.85
3. Cicatrização de ferimentos	616-003.9

Catalogação na fonte elaborada pela bibliotecária
Carolina Machado Quadros – CRB 10/2236.

A BUSCA DE MEDIADORES PARA A MODULAÇÃO DE COLÁGENO: EFEITO DE MOLÉCULAS ATIVAS INCORPORADAS A BIOMATERIAL POLIMÉRICO

Anderson Ricardo Ingracio

Defesa: 03 de Julho de 2018

Banca examinadora:

Orientação Prof. Dr. Asdrubal Falavigna

Prof. Dr. Daniel Marinowic

Prof. Dr. Darcy Ribeiro Pinto Filho

Prof. Dr. Luciano da Silva Selistre

UNIVERSIDADE DE CAXIAS DO SUL

PROGRAMA DE PÓS-GRADUAÇÃO EM CIÊNCIAS DA SAÚDE

COORDENADOR DO PROGRAMA DE PÓS-GRADUAÇÃO EM CIÊNCIAS DA SAÚDE

PROF. DR. ASDRUBAL FALAVIGNA

Dedicatória

Dedico esta obra à minha filha amada, Bia. A maior inspiração dos meus esforços, a razão dos meus pensamentos. Carrego você comigo, em meu coração. Eu não existo longe de você.

Agradecimentos

Ao meu orientador **prof. Dr. Asdrúbal Falavigna**, pelo apoio, incentivo, paciência e sabedoria prestados a mim durante essa jornada. Um especial agradecimento à sua família, por vezes privada de sua companhia para meu benefício.

Ao meu co-orientador **prof. Dr. Otávio Bianchi**, por toda orientação no estudo de uma área estranha à minha formação médica. Sua parceria foi essencial para o desenvolvimento deste trabalho.

Ao **prof. Dr. Luciano Selistre**, pelo auxílio inestimável na construção da análise estatística de meus resultados, sem a qual meus esforços não agregariam conhecimento científico.

Às **Dras. Manuela Figueiró** e **Natália Fontana Nicoletti**, presenças incondicionais ao longo desse período, agregando experiências e conhecimentos em todos os momentos deste estudo. Por terem cuidado dos detalhes desta obra com toda dedicação e entusiasmo possíveis. Pelo apoio e incentivo nos momentos de dificuldades. Tenham certeza de que foram essenciais.

À **Dra. Fernanda Trindade Gonzalez Dias** por sua disponibilidade e inestimável colaboração na área da engenharia, imprescindíveis a essa pesquisa.

À **Dra. Karina Salgado**, ICAP – Laboratório de Patologia, e às biomédicas **Bruna** e **Jéssica**, pela ajuda e orientação na confecção do material histológico, dedicando seu tempo e seu empenho a este projeto.

Ao **prof. Gabriel Pauletti**, Instituto de Biotecnologia – Laboratório de Entomologia, e aos **bolsistas do laboratório**, pela disponibilidade de sua estrutura e pela orientação e ajuda sempre que necessários.

Ao **prof. Wilson Sampaio de Azevedo Filho**, Agronomia – Laboratório de Entomologia, pela disponibilidade de sua estrutura e por sua colaboração e orientação.

À veterinária **Caroline Nesello** e às biólogas **Simone Andriolo Gross** e **Raquel Brandalise**, por sua dedicação e auxílio durante os procedimentos e pelo carinho que dispensaram aos animais envolvidos, indispensáveis nesse estudo.

Aos **professores desta pós-graduação**, representando os professores envolvidos em todos os níveis de minha formação, por seu carinho e dedicação em ensinar, nem sempre valorizados com a devida importância. Minhas virtudes são reflexo dos seus ensinamentos; minhas imperfeições, falhas em receber tudo aquilo que me era ensinado.

Aos **meus alunos**, de agora e de outrora, pela compreensão e ajuda em me tornar um bom professor.

Aos meus pais, **Ceres** e **Roberto**, por me propiciarem os maiores ensinamentos da vida, os valores humanos que uma boa pessoa e um bom profissional jamais deve esquecer.

À minha esposa **Bruna** e à minha filha **Bia**, pela compreensão nos momentos de ausência durante uma jornada que não era sua.

À minha **família** e **amigos**, representados pelos meus tão queridos irmãos **Cassiano**, **Mozar** e **Christian**, por sua incondicional parceria e aconchego.

À **Deus**, por todas oportunidades, por todas as pessoas que me cercam.

Sumário

Esta dissertação de Mestrado Acadêmico Stricto Sensu é apresentada no formato exigido pelo Programa de Pós-Graduação em Ciências da Saúde da Universidade de Caxias do Sul. A mesma é constituída da secção de “Introdução com referências bibliográficas”, a inclusão do artigo original submetido/publicado em periódico Qualis A na classificação da Coordenação de Aperfeiçoamento de Pessoal em Nível Superior (CAPES), e as “Considerações Finais e Perspectivas

1 INTRODUÇÃO

A cicatrização tecidual, elemento comum a todas as linhagens histológicas, é uma sequência de eventos celulares e moleculares que visa cessar o dano e reparar os tecidos, a fim de restaurar sua estrutura anatômica, aspecto e funcionalidade [1-3]. Diferentemente da regeneração tecidual, de ocorrência incomum em humanos, a cicatrização gera alterações teciduais que a diferencia dos tecidos originais [4]. Quanto menor a diferença entre as características do tecido original e aquele obtido após cicatrização, menor o impacto em sua funcionalidade [1, 3, 4]. Independente do tecido histológico lesado, a matriz extracelular (ME) constitui o arcabouço anatômico que confere sua resistência [2, 5]. A ME é composta pelo conjunto de células, proteínas e moléculas localizadas no espaço intersticial, se caracterizando por ser um ambiente rico em fatores de crescimento (FC), com importante papel modulador na angiogênese e desenvolvimento tecidual [1, 4, 5]. As longas e densas fibras de colágenos desempenham uma função essencial na resistência tecidual e na interação entre a célula e a ME [3, 4, 6, 7]. Durante o processo de remodelamento da ferida há a substituição das fibras de colágeno, onde um equilíbrio entre sua síntese (neoformação) e apoptose (lise) determina o resultado final do processo cicatricial e a formação da ME [1, 2, 5, 7]. Essa sequência de eventos é mediada por fatores de crescimento [4, 7].

O plasma rico em plaquetas (PRP) é um produto do sangue autólogo, que atua no reparo tecidual por apresentar uma elevada concentração de plaquetas e uma grande variedade de fatores de crescimento [8]. A função plaquetária é amplamente conhecida e estabelecida no processo de hemostasia, por formação da rede de fibrina, e pelo seu efeito secretor pró-coagulação [4, 9-11]. Posteriormente, sua função secretora endógena de modulação do processo cicatricial, desempenhada pelos grânulos alfa, passou a ser conhecida [8, 11, 12]. O termo PRP foi claramente utilizado para a modulação do reparo tecidual em 1998, por Marx [13, 14]. O PRP é definido como um elevado concentrado de plaquetas, se comparado aos níveis plaquetários do sangue total, com uma maior densidade de fatores de crescimento [8, 14, 15]. Não está estabelecido na literatura a concentração de plaquetas necessária para que seja reconhecido como PRP, sendo aceitos níveis plaquetários entre 3 a 4 vezes as

contagens basais como índices mínimos [8, 14-16]. O PRP passou a ser reconhecido como uma solução rica em FC tecidual e utilizado na tentativa de aprimorar o processo cicatricial [8, 11, 16, 17]. Ainda que não exista informação definitiva sobre a atuação do concentrado de plaquetas relacionada à via específica modulada ou à fase em que ocorra, a aplicação no sítio da lesão tecidual do PRP tem sido proposta, inclusive com a utilização de polímeros, pela facilidade de associação a biomateriais.[17]

Em procedimentos da coluna vertebral, o processo cicatricial possui especial relação com o desfecho clínico. Mesmo que sutis, deposições pós-operatórias de colágeno local, podem desencadear um novo processo patológico [18]. O aumento na deposição de colágeno, associado a alteração na arquitetura histológica, pode levar à fibrose [5]. No caso das cirurgias vertebrais, podem desencadear uma retração ou compressão tecidual de difícil resolução clínica [19]. A fibrose epidural é uma complicação comum em cirurgias de intervenção com abertura do canal vertebral [18, 20]. A inibição da formação de fibrose epidural, pela aplicação de fatores moduladores do processo cicatricial, melhora o sucesso terapêutico. Como barreiras para sua aplicabilidade, existe a dificuldade de alcançar um número efetivo de fatores de crescimento no local da injúria.

Os biomateriais tem sido utilizados como método diagnóstico e terapêutico [21]. Nanomembranas de poliamida vem sendo testados como arcabouços bioativos e propícios à engenharia de tecidos [22-24]. A elevada razão superfície/volume e a estrutura porosa do material, favorece à proliferação e diferenciação celular, o transporte de nutrientes e à excreção de metabólitos entre a matriz da fibra e o ambiente externo [25]. A poliamida-6 comercializada (PA6) é um polímero sintético e biocompatível, aprovado pelo órgão regulamentador *Food and Drug Administration* (FDA) para uso em humanos e bastante utilizado clinicamente em suturas cirúrgicas [26]. Quando aditivado com óleo de soja maleinizado (SOMA), este polímero se torna bastante tenaz, característica importante para o manuseio e morfogênese celular do suporte polimérico [27]. A associação de FC e/ou PRP a nanomembranas de poliamida seria uma alternativa para aplicação de maneira tópica em localizações anatômicas desfavoráveis. Somado a isso, um carreador que promova um suporte às

biomoléculas, passa a proteger o tecido, impedindo sua degradação rápida pela ação das proteases.

O resultado prático do efeito do PRP na cicatrização é objeto de estudo científico. Duas revisões sistemáticas mostraram como desfecho primário uma variável, por vezes subjetiva, como cicatrização completa, formação de calo ósseo ou quantidade de sangramento, sem analisar o motivo pelo qual estes resultados aconteceram [12, 28]. Estudos de baixo nível de evidência, em animais e *in vitro,* descrevem o PRP como modulador positivo da cicatrização [11, 12]. A literatura não permite estabelecer o real efeito do PRP nas fases de reparação celular, formação de colágeno ou deposição de matriz extracelular.

O presente estudo visa analisar o efeito da aplicação tópica de PRP e do FC recombinante humano PDGF-BB na deposição de colágeno tipos I e III utilizando uma matriz polimérica carreadora. A PA-6/SOMA teria as funções de proteger as moléculas biológicas (FC) das proteases, abundantes na ferida em cicatrização, e atuar como barreira física no tecido lesado. Além disso, considerando suas propriedades demonstradas em estudo *in vitro*, a PA-6/SOMA permitiria meia vida aumentada e liberação controlada do FC no sítio alvo, auxiliando sua atuação na modulação da deposição de colágenos tipo I e III. Desta forma, a PA-6/SOMA assumiria papel de matriz carreadora ativa no processo de remodelação tecidual, contribuindo para a prevenção de processos patológicos como a fibrose.

2 REFERÊNCIAS

1. Velnar T, Bailey T, Smrkolj V. The wound healing process: an overview of the cellular and molecular mechanisms. J Int Med Res. 2009;37(5):1528-42.
2. Janis JE, Harrison B. Wound Healing: Part I. Basic Science. Plast Reconstr Surg. 2016;138(3 Suppl):9s-17s.
3. Gonzalez AC, Costa TF, Andrade ZA, Medrado AR. Wound healing - A literature review. An Bras Dermatol. 2016;91(5):614-20.
4. Reinke JM, Sorg H. Wound Repair and Regeneration. European Surgical Research. 2017;49(1):35-43.
5. Diegelmann RF, Evans MC. Wound healing: an overview of acute, fibrotic and delayed healing. Front Biosci. 2004;9:283-9.
6. Shah JMY, Omar E, Pai DR, Sood S. Cellular events and biomarkers of wound healing. Indian J Plast Surg. 2012;45(2):220-8.
7. Baum CL, Arpey CJ. Normal cutaneous wound healing: clinical correlation with cellular and molecular events. Dermatol Surg. 2005;31(6):674-86; discussion 86.
8. Anitua E, Andia I, Ardanza B, Nurden P, Nurden AT. Autologous platelets as a source of proteins for healing and tissue regeneration. Thromb Haemost. 2004;91(1):4-15.
9. Kasahara K, Souri M, Kaneda M, Miki T, Yamamoto N, Ichinose A. Impaired clot retraction in factor XIII A subunit-deficient mice. Blood. 2010;115(6):1277-9.
10. Farrior E, Ladner K. Platelet gels and hemostasis in facial plastic surgery. Facial Plast Surg. 2011;27(4):308-14.
11. Nurden AT, Nurden P, Sanchez M, Andia I, Anitua E. Platelets and wound healing. Front Biosci. 2008;13:3532-48.
12. Smyth NA, Murawski CD, Fortier LA, Cole BJ, Kennedy JG. Platelet-rich plasma in the pathologic processes of cartilage: review of basic science evidence. Arthroscopy. 2013;29(8):1399-409.
13. Marx RE, Carlson ER, Eichstaedt RM, Schimmele SR, Strauss JE, Georgeff KR. Platelet-rich plasma: Growth factor enhancement for bone grafts. Oral Surg Oral Med Oral Pathol Oral Radiol Endod. 1998;85(6):638-46.
14. Marx RE. Platelet-rich plasma (PRP): what is PRP and what is not PRP? Implant dentistry. 2001;10(4):225-8.
15. Dhurat R, Sukesh M. Principles and Methods of Preparation of Platelet-Rich Plasma: A Review and Author's Perspective. J Cutan Aesthet Surg. 2014;7(4):189-97.
16. Alsousou J, Thompson M, Hulley P, Noble A, Willett K. The biology of platelet-rich plasma and its application in trauma and orthopaedic surgery: a review of the literature. J Bone Joint Surg Br. 2009;91(8):987-96.
17. Anitua E, Tejero R, Alkhraisat MH, Orive G. Platelet-rich plasma to improve the bio-functionality of biomaterials. BioDrugs. 2013;27(2):97-111.
18. Sae-Jung S, Jirarattanaphochai K, Sumananont C, Wittayapairoj K, Sukhonthamarn K. Interrater Reliability of the Postoperative Epidural Fibrosis Classification: A Histopathologic Study in the Rat Model. Asian Spine J. 2015;9(4):587-94.

19. Bosscher HA, Heavner JE. Incidence and severity of epidural fibrosis after back surgery: an endoscopic study. Pain Pract. 2010;10(1):18-24.
20. Akeson WH, Massie JB, Huang B, Giurea A, Sah R, Garfin SR, et al. Topical high-molecular-weight hyaluronan and a roofing barrier sheet equally inhibit postlaminectomy fibrosis. Spine J. 2005;5(2):180-90.
21. Langer R, Tirrell DA. Designing materials for biology and medicine. Nature. 2004;428(6982):487-92.
22. Nair LS, Laurencin CT. Polymers as biomaterials for tissue engineering and controlled drug delivery. Adv Biochem Eng Biotechnol. 2006;102:47-90.
23. Vasita R, Shanmugam IK, Katt DS. Improved biomaterials for tissue engineering applications: surface modification of polymers. Curr Top Med Chem. 2008;8(4):341-53.
24. Ravichandran R, Sundarrajan S, Venugopal JR, Mukherjee S, Ramakrishna S. Advances in polymeric systems for tissue engineering and biomedical applications. Macromol Biosci. 2012;12(3):286-311.
25. Zeltinger J, Sherwood JK, Graham DA, Mueller R, Griffith LG. Effect of pore size and void fraction on cellular adhesion, proliferation, and matrix deposition. Tissue Eng. 2001;7(5):557-72.
26. Maitz MF. Applications of synthetic polymers in clinical medicine. Biosurface and Biotribology 2015;1:16.
27. Ernzen JR, Bondan F, Luvison C, Wanke CH, Martins JDN, Fiorio R, et al. Structure and properties relationship of melt reacted polyamide 6/malenized soybean oil. Journal of Applied Polymer Science. 2016.
28. Eppley BL, Pietrzak WS, Blanton M. Platelet-rich plasma: a review of biology and applications in plastic surgery. Plast Reconstr Surg. 2006;118(6):147e-59e.

3 ARTIGO

Article type: Regular Article

Towards on the Mediators in Collagen Replacement: Effect of the Active Molecules into a Polymeric Biomaterial

Anderson Ricardo Ingracio[1], Natália Fontana Nicoletti[2], Fernanda Trindade Gonzalez Dias[3], Manuela Figueiró[2], Otávio Bianchi[1,3], Asdrubal Falavigna[1,2]

[1] Health Sciences Graduate Program, Universidade de Caxias do Sul (UCS), Caxias do Sul, RS, Brazil
[2] Cell Therapy Laboratory (LATEC), Universidade de Caxias do Sul (UCS), Caxias do Sul, RS, Brazil
[3] Materials Science Graduate Program (PGMAT), Universidade de Caxias do Sul (UCS), Caxias do Sul, RS, Brazil

Running title: Potential mediators in collagen replacement

Corresponding author:
Asdrubal Falavigna MD, PhD
Laboratory of Basic Studies on Spinal Cord Pathologies
Department of Neurosurgery, University of Caxias of Sul
Coordinator of Post-Graduation Program in Health Science.
Caxias do Sul, Rio Grande do Sul 95070-560, Brazil
E-mail: asdrubalmd@gmail.com

Abstract

Modulating healing factors could avoid or minimize some possible pathological processes in collagen deposition. The present study was aimed to evaluate the role of active biomolecules such as PDGF-BB and PRP loaded or not into polymeric biomaterial to seek potential mediators in types I and III collagen deposition and epithelization. The healing phases was investigated by using an *in vivo* full-thickness wound rat model. At zero, 3rd, 7th and 14th days after the experimental model, the size of the wound areas was photographed. The nanofibrous materials were biocompatible and did not cause any local adverse reaction and/or inflammation. On day 14 the wounds had healed almost 100% with better signs of healing, however there was no obvious difference in the wound contraction rates. At the end of 14 days, samples from the center of the lesion were collected when histological features and immunopositivity for collagen I and III expression were assessed. There was no significant difference in the epithelization among the groups. Wounds treated with PRP and with PA-6/SOMA plus PDGF-BB had significantly lower amounts of type III collagen. The amounts of type I collagen did not have a statistically different deposition among the experimental groups. The association of PDGF-BB with PA-6/SOMA emerges as an alternative for topical application to unfavorable anatomical sites, suggesting that these association may have a positive modulation on the process of accelerated healing remodeling.

Keywords: Collagen; fibrosis; platelet-rich plasma; polyamide-6 and biomaterial.

Introduction

Tissue healing is a dynamic and coordinated sequence of cellular events common to all histological lines to restore their anatomical structure, appearance and functionality [1-3]. Unlike regeneration, unusual in mature human tissue, healing evokes tissue changes that distinguish it from the original histological tissue features [4]. The smaller the difference between the tissue characteristics and those present after healing, the lower the impact on its functionality [1, 2, 4].

Regardless of damaged tissue, the extracellular matrix (ECM) has a decisive role and constitutes the anatomical framework that confers resistance [2, 5]. This matrix is characterized by an abundant growth factors (GF) environment that modulates angiogenesis and tissue development [1, 4, 6]. Long and dense collagen fibers play an essential role in tissue resistance and in the interaction between resident cells, soluble mediators and ECM molecules [3, 4, 6]. In this sense, collagen synthesis is a pivotal event in the physiological cicatricial process, since deficient deposition and/or altered lysis can disrupt the course of wound healing [2, 5]. Increased collagen deposition, associated with an alteration in histological architecture, leads to the progression of the pathological process known as fibrosis [5]. Fibrosis is an expected event in invasive procedures, but its intensity can induce a retraction and dysfunction of anatomical structures [7, 8]. A classical phenomenon is the symptomatic retraction of spinal epidural fibrosis that triggers chronic neuropathies with high refractoriness to pharmacological or surgical treatment [7, 9, 10].

To improve the application of modulating factors in specific anatomical sites, it is necessary to study the ideal method for local delivery of biomolecules. One approach includes direct deposition of the biomolecule at the wound site, while another considers the use of a biomaterial as a carrier vehicle for local release. It is known that the administration of these biological agents may lead to some undesirable events, such as rapid degradation by proteases in the wound environment [11]. GF that are currently approved by the US Food and Drug Administration (FDA) have been used as some form of delivery system [12]. Controversially, platelet-rich plasma (PRP) is commonly used by direct application into wound site and there is no consensus about its performance as a specific modulator in the healing phases [13].

The advantages of using biomaterials as delivery vehicles are that biomolecules can be protected from endocytosis and have structural support on which the host cells can migrate to facilitate tissue regeneration. A nanofibrillar scaffold based on a synthetic polymer was chosen to be tested as a system for topical biomolecule delivery in this study. Polyamide-6 (PA-6) is a

FDA-approved polymer for human use in surgical sutures, especially for its structural similarity with proteins [14]. When chemically modified with maleinized soybean oil (SOMA), PA-6 becomes very tenacious, which favors biomaterial handling and cellular morphogenesis [15]. PA-6/SOMA scaffolds showed superior biocompatibility and an intriguing 3D architecture, as attested in a previous work by our group [16]. PA-6/SOMA biomaterial also exhibited a covalent-binding interaction with PDGF-BB, which may contribute to the controlled-release of the biomolecules.

The present study aimed to evaluated the collagen deposition and epithelization during the healing phases by using an *in vivo* wound healing model to verify the role of active biomolecules such as PDGF-BB and PRP loaded or not into PA-6/SOMA. This work focused on the influence of the strategy chosen for biomolecule administration in order to evaluate possible modulations in contraction rates and collagen type III to type I replacement in full thickness wounds to handle the fibrosis response after tissue injury.

2. Materials and Methods

2.1 Animals

Male Wistar rats (200-300 g; N=36), were obtained from the Federal University of Rio Grande do Sul (UFRGS). During the set of experiments, the animals were kept in the Laboratory of Animal Physiology and Experimentation at the University of Caxias do Sul (UCS). All the experimental procedures following the Brazilian Guideline for Care and Use of Animals for Scientific and Educational Purposes (MCTI, CONCEA, DBCA, 2013) and the recommendations for laboratory animal care and ethical standards for experimental animal testing in the National Institute of Health (NIH) Laboratory Use and Care Guide. All the experimental protocols were approved by the local Animal Ethics Committee (CEUA-UCS; protocol number: 017/2016).

The animals were housed in cages under conditions of optimum light, temperature and humidity (12 h light-dark cycle, 22±1°C, under 60 to 80 % humidity). Animals received pelleted rodent feed and filtered water *ad libitum*. No experimental procedure was performed in the room where the animals were maintained, to avoid any type of behavioral stress. In the postoperative period, animals were maintained on a thermal mattress until recovery and housed in individual cages. Analgesia was performed by administering tramadol (5 to 7.5 mg/ kg, s.c.) every 12 hours for 3 to 5 days as individually needed. The animals were euthanized by isoflurane overdose fourteen days after the procedure, when the skin wound was completed.

2.2 Study design: Full-thickness *in vivo* wound model

The animals were anesthetized with ketamine hydrochloride (80mg/kg) mixed with xylazine (10mg/kg) intraperitoneally. After trichotomy, the animals were positioned in ventral decubitus and the areas of dorsal lesions were measured and demarcated. Concerning the dorsal midline, each animal was subjected to two full-thickness incisional circular cutaneous resections, 1 cm in diameter using a cutaneous punch until the dorsal muscular fascia was exposed. There was a 1.5 cm separation between the lesion areas to prevent contact and possible extravasation of the active biomolecule. The procedures were carried out by the same operator to avoid technique variations. A different experimenter randomly allocated the animals into the different groups.

Animals were randomly divided into the following experimental groups (N = 6 per group): (i) control/PDGF-BB group; (ii) PA-6/SOMA + PDGF-BB group; (iii) PA-6/SOMA +

PRP group. The *control/PDGF-BB group* received no application to the left lesion (L) and received the application of PDGF-BB only to the right lesion (R). In the *PA-6/SOMA + PDGF-BB group*, the polyamide nanomembrane alone was placed inside lesion L, while the biomaterial loaded with PDGF-BB was kept in lesion R. The *PA-6/SOMA + PRP group* received PRP in lesion L and PA-6/SOMA plus PRP in lesion R (Figure 1). No membranes applied to on the wounds were sutured to the skin. The wound sites were observed macroscopically within a 14-day follow-up.

2.3 Platelet-rich plasma (PRP)

Whole blood (6 mL) was collected by cardiac puncture from donor animals by using an anticoagulant in a proportion of 20% of the total blood volume. The blood was centrifuged for 10 minutes at 1000 rpm to separate the plasma and hemocyte fraction. The plasma fraction and the mist zone were transferred to a new tube and centrifuged for 10 minutes at 1600 rpm. Three distinct layers were obtained and the intermediate layer, designated as PRP, was collected. The mean number of platelets in whole blood of PRP-donor rats was 896 x 10^3 platelets/μL. After PRP preparation, the platelet count was 340 x 10^4/μL producing a 3.8-fold increase in concentration compared to native plasma. The number of platelets of each PRP fraction was counted by using a hemocytometer to reach a concentration of 10,000 platelets/μL. Next, 20 μL of the fresh PRP was used on cutaneous wounds topically, injected into the center of the lesion, or incorporated into PA-6/SOMA nanomembrane.

2.4 Recombinant human PDGF-BB

Recombinant human platelet-derived growth factor-BB (PDGF-BB) (Pepro Tech Inc., Rocky Hill, NJ) was reconstituted in 0.1% BSA and diluted with ultra-pure water to achieve a concentration of 10 μg/mL and stored at -80ºC. PDGF-BB (100 ng) in solution was directly injected into the center of the lesion or added to PA-6/SOMA nanomembrane and incubated for 45 minutes at 37ºC.

2.5 PA-6/SOMA nanomembrane as a carrier vehicle

A chemically modified PA-6 (PA-6/SOMA) was tested as a carrier agent of the biological factor (PDGF-BB or PRP) to assess its benefit for topical delivery, as well as wound healing. PA-6/SOMA nanomembrane was produced by electrospinning technology, from

polymeric solutions under the experimental conditions: 0.1 ml/h feeding rate, 15 cm syringe-collector distance and 25 kV applied voltage. The electrospinning process and the structure of this nanomembrane are represented in Figure S1 (see in supplementary files). The PA-6/SOMA mats were composed of uniform nanofibers with the diameter (250.0 ± 9.0 nm) within range of extracellular matrix collagen fibers (ECM). Dias et. al (2017) [16] thoroughly discussed the properties of PA-6/SOMA scaffold.

2.6 Morphometric analysis

At zero (lesion time), 3rd, 7th and 14th days after the experimental model, the size of the wound areas was photographed on a perpendicular by means of a digital camera (Fujifilm Finepix HS10) with 35 mm lens aperture and 27.5 cm distance between lens and bench under the same conditions each time. The analysis of the non-epithelial lesions in the pictures was marked and the number of pixels within the bordered area was measured to calculate the wound area by using Image J-Pro Plus 4.0 software (Media Cybernetics L.P). The wound area contraction rate (C) was calculated based on the measured area on day zero (A0; postoperative) and the area reduction rate on the 14th day (A14), through the following expression: C = A0 - A14. The rate of cicatricial contraction (TC) was determined from the previous results by means of TC = C x 100 / A0.

2.7 Histological analysis

After the 14-day follow-up, samples from the center of the lesion were collected and immediately fixed in 10% formaldehyde for further processing and analysis. Serial sections of 5 μm were stained with hematoxylin and eosin (HE). Histological observation and measurements of the presence or absence of reepithelialization were performed under a light microscope (Leica DM2500, Leica Microsystems, Bannockburn, IL, U.S.A.) equipped with an automated Leica digital camera system (Leica DMC2900, Leica Microsystems) and an image manager software (LASV4.4, Leica Microsystems). The analyses were performed by an experimenter blinded to the experimental groups.

2.8 Immunohistochemistry

Immunopositivity for collagen I and III expression were assessed on paraffin tissue sections (3-μm thick) by using polyclonal rabbit anti-collagen I (1:100, Cat #ab34710, abcam, Cambridge, United Kingdom), and polyclonal rabbit anti-collagen III (1:50, #ab7778, abcam,

Cambridge, United Kingdom), according to the procedures previously described [17]. Images were examined with a Leica DM2500 light microscope (Leica Microsystems, Bannockburn, IL, U.S.A.). Four images of each wound lesion were captured in x200 magnification. To quantify the immunopositive collagen I and III, digitized RGB images were analyzed using Image NIH Image J 1.36b Software (NIH, Bethesda, MD, USA). For this purpose, a specific macro was created for each sample to quantify the collagen type immunopositivity based on pixel color. The dark-to-medium brown regions in the sample were selected and used as positive immunolabeling. The software generated a macro, which allowed determining the optical density of the positive regions.

2.9 Statistical analyses

Data from experimental results were statistically processed using program R version 3.4.4., considering 5% significance (α) and 90% statistical power. A difference of standardized means greater than or equal to 1.5 standard deviation units between groups (E / S≥1.5) was detected. The morphometric results between groups were compared through a linear mixed model for repeated measures with localization of Tukey's post-hoc test. The variance of measures compared the concentration of collagen (histomorphometric analysis).

3. Results

3.1 Clinical aspects and macroscopic evaluation of the wound

The cutaneous wound was macroscopically evaluated *in vivo* during 14 days. The wound site presented a homogenous surface without signs of granulation tissue exposure and developed a crust adhered to the injury site from the 3rd-day post procedure. The wound edges retracted regularly in all animals and at 14 days the wounds were almost completely healed. The response of the wound site denoted that the presence of the nanofibrous carrier did not cause any local adverse reaction and/or inflammation, as did also, the direct application of PDFG-BB or PRP into the center of the wound site (Figure 2a). In the wounds in which the biomaterial was applied, also there was the formation of a neat crust on and around it, leading to the creation of an interfacial tissue that was later incorporated by the newly tissue formed. The biomaterials remained fixed at the wound site the entire time and did not need sutures to keep them in position.

3.2 Wound closure

Photographic images of the wound healing progress were captured at four points in time (0, 3, 7 and 14 days) and are summarized in Figure 2a. There was no noticeable difference in the speed of wound contraction among the animals treated by PDGF-BB or PRP loaded or not in PA-6/SOMA at the specified times. A marked improvement was seen after 7 days post-procedure when the injuries became covered by a solid, intact and dark brown scab. Thenceforward, the wounds started to slough off leaving behind minimal crust remnants in predominantly epithelized wounds that become progressively smaller. On day 14 the wounds were almost closed, achieving nearly 100% of closure with better a sign of healing (Figure 2b-c; Table 1). It is important to emphasize that the physical strength generated by the biomaterial application on the wound site did not delay wound contraction.

3.3 Histological findings

Epithelization is an essential component of wound healing used as a defining parameter of successful wound closure. The epithelized areas at the wound were easy to see from the images of HE-stained sections. There was no significant difference in the epithelialization among the groups, suggesting that they did not accelerate the epithelization of full-thickness

skin defect wounds in a 14-day follow-up period (Table 1). However, the physical presence of the biomaterial did not inhibit the epithelization rates too.

3.4 Collagen I and III

Deposition of type I and type III collagen was measured at 14 days follow-up. This event corresponds to the phase of cicatricial remodeling in rats, initiated about 10 days after the injury. In this phase, there should be the exchange of collagens, with the replacement of collagen type III by collagen type I. In absolute numbers, it was observed differences in the collagen deposition of the groups in relation to the control. A tendency to smaller amplitude of difference between the two types of collagen was observed in the groups treated with PA-6/SOMA. Wounds treated with PRP and PDGF-BB-loaded PA-6/SOMA had lower amounts of type III collagen. The amounts of type I collagen did not have a statistically different deposition between the groups compared to the control group. The difference in the amount of type III collagen is especially crucial in the PDGF-BB-loaded PA-6/SOMA. The result found for isolated PRP was not replicable when this biological factor was associated with PA-6/SOMA. A smaller amount of type III collagen, without loss of type I collagen deposition, is the primary finding of the cicatricial remodeling process.

4. Discussion

Every tissue disruption with consecutive loss of organ functions might be described as a wound and it is necessary to be able to rely on clinically efficient healing whenever a patient receives surgical intervention. If the surgical wound healing fails to progress in a timely and orderly fashion to repair the injured tissue it leads to an unspecified form of closure and causes fibrosis and scar formation [1].

The present work used a biomaterial consisting of polymeric nanofibers as a vehicle to improve the local application of PRP and PDGF-BB. Concerning the topical application of PA-6/SOMA to the wounds, two topics are especially considered: if the biomaterial was effective in delivering the biological compounds locally and if its their presence *per se* did not negatively alter the process. According to the results, both PDGF-BB and PRP applied alone or in association with PA-6/SOMA presented the same healing rates. Natural and synthetic polymers have been used for biomolecule delivery in *in vivo* animal wound healing studies. Compared with cellular scaffolds, these polymeric matrices exhibit better ECM formation although no significant changes in healing rates [18, 19, 20]. A controlled release of bFGF and EGF biomolecules incorporated in synthetic polymers promoted faster wound closure in 14 days [21, 22]. Of note, the physical strength generated by the PA-6 based biomaterial application on the wound site did not undermine the healing process, which confirms the potential of PA-6/SOMA being applied as a vehicle for topical delivery. This feature is a pivotal point considered to create polymeric textiles for drug delivery aiming at tissue repair and healing.

Satisfactory wound contraction was achieved by using natural products and cell sources but without being hampered by a scaffold, when its physical presence might be precluded wound contraction [23, 24]. In this sense, the same animal studies also had demonstrated accelerated healing when the wound bed was supplied by GF or PRP. Incorporation of PDGF-BB or PRP in PA-6/SOMA biomaterial would be an alternative for topical application at unfavorable anatomical sites. Also, a carrier that supports biomolecules becomes a protective factor, preventing simultaneously their rapid degradation by proteases and diffusion in the wound environment.

PDGF presents wound healing activities in both bone and soft tissue. Currently, the only FDA approved GF is the human recombinant PDGF-BB [25]. The commercially available formulations of PDGF-BB use a high concentration (100 µg/ml) in order to heal wounds effectively. This high concentration likely leads to elevated systemic levels of GF that may

drive adverse reactions. Therefore, wound dressings that improve the efficacy of PDGF-BB have a great potential in postsurgical wound complications. PRP is defined as a higher concentrate of platelets when compared to whole blood levels, presenting a higher density of GF [11, 26, 27]. Platelet function is widely known and established in hemostasis [4, 10, 13], the principal standpoint of the perfect healing. The platelets concentration necessary to be recognized as PRP has not been established and a platelet level 3 to 4 times that of whole blood is well accepted [11, 13, 26, 27]. In our study, it was followed previous recommendations for PRP manufacture and the methodology applied was achieved, with a supply of autologous concentrate rich in GF.

The soybean oil derivative chains of PA-6/SOMA are constituted by fatty acids and tocopherols, related to anti-inflammatory and epithelizing properties which makes it a possible wound-healing accelerator. At first, the PDGF-BB and PRP used alone or in combination with this biomaterial were not able to modulate the epithelization on the healing process. Although epithelization is an essential component of wound healing used as a defining parameter of its success, the difference seen between samples can be understood by the amplitude that the correct measurement of its physiological characteristics, considering its papillary projections, needs to be contemplate.

PA-6/SOMA did not degrade by physiological process of cells and spread of tissue fluids over the 14 days of follow-up. In time, the body breaks down the biomaterial and only a newly formed skin layer should remain. Some intracellular fragments of a dermal polymeric scaffold were detected by electronic microscopy in five patients with burn injury one-year post-treatment [28]. The presence of these fragments indicated that cells could phagocytize the biomaterial and that it did not cause any adverse reaction in the organism. This justifies the advantage of a slow-degradable biomaterial, in addition to its mechanical support that guarantees the tissue ingrowth.

Closely related to proper ECM deposition is the degree of wound contraction. During the wound remodeling process, there is a replacement of collagen fibers, such that quality of ECM cicatricial process results from the balance between its neoformation and lysis (1, 2, 5, 6). Collagen I must gradually replace collagen III to increase mechanical stability of the tissue and resist over-contraction by myofibroblasts, which is associated with pathological scarring [29].

Increasing the rate of wound closure is not necessarily an improvement in itself. PDGF-BB-loaded PA-6/SOMA showed positive modulation on tissue remodeling by collagen

replacement. This event is considered a key on healing acceleration in different histological lines [18, 21, 30]. The deposition of dermal collagen, even as an isolated measure, can be correlated with the activity of pathological processes in parallel with the marker function proposed in the tissue repair events [29]. When not part of the healing process, its modulation may not interfere with clinical outcome.

Collagen III levels are generally up-regulated in the early phase of wound healing and mechanically poor tissues [31]. The down-regulation of collagen III at 14 days post-injury in rats treated with PDGF-BB-loaded PA-6/SOMA indicates good mechanical tissue properties. Furthermore, the increased density of type I collagen would probably continue beyond 14 days if the animal model follow-up had been extended, suggesting rapid and continuous collagen replacement from type III to type I. A previous animal study with wounds topically treated with lavender oil demonstrated that suppression of type III collagen in the wound area enhanced myofibroblast expression and differentiation to promote wound contraction [24, 32]. Polymeric biomaterial coated with bFGF allowed the controlled release of the biomolecule and led to a significant enhancement of collagen I density in addition to better elastin and collagen structure in diabetic rats submitted to a full-thickness wound [21, 22]. Using the same animal model, a recent study took an advanced approach to enable controlled release of a combination of GF (EGF, VEGF and PDGF) incorporated in natural polymers to improve both collagen content and remodeling rates [33].

The assessment of the histological state of the healing is essential in clinical practice for postoperative management. Epidural fibrosis is probably inevitable after any surgery that involves manipulation of the epidural space. Based on preclinical and clinical research, this epidural scarring may be the causative to persistent pain as a consequence to nerve roots compression and might reduce the ability of the spinal structures to cope with degenerative changes [8, 9]. Subsequent perineural fibrosis may interfere with cerebrospinal fluid mediated nutrition, resulting in hypersensitivity of nerve roots [7]. New studies would be proposed to prevent epidural fibrosis by avoiding primary factors rather than applying particular drugs or materials [10].

Nanofiber scaffolds produced by electrospinning mimic the 3D fibrous structure of native ECM and offer the ability to incorporate biological factors that promote regeneration [34, 35]. PA-6/SOMA scaffolds have the permeable required background provides the necessary humidity and probably offers the sustained release of the PDGF-BB, which might explain the

better support to collagen replacement by the PDGF-BB-loaded PA-6/SOMA system in this study. An optimal system for biomolecule delivery has to meet some requirements, such as non-cytotoxic, mechanical strength and elasticity, and a degradation rate that supports initial tissue formation, but does not hinder maturation of the regenerated tissue due to delayed resorption.

Despite the importance of collagen deposition for repair, practical results of PRP and GF effects on healing are the subject of studies. Two systematic reviews showed that outcomes of articles were a clinical variable; for example, complete healing, bone callus formation or amount of bleeding, without examining the reasons why these results occurred [36, 37]. Despite low-level evidence animal studies and *in vitro* experiments describing a positive modulating effect of healing, the literature does not allow establishing the real impact of PRP or GF on cell repair phases, collagen formation or extracellular matrix deposition [36, 38-40]. Although the parameters of most scoring systems are based on basic knowledge of the healing, the parameters chosen in this experimental model focus on the scientific question underlying the hypothesis and the pathogenesis of wound healing. The set of experiments that compose this work considered the deposition of collagen a beneficial factor in the healing process but did not correlate orientation and organization of collagen fibers nor did it measure considerable patterns of tensile strength.

The association of PDGF-BB with PA-6/SOMA emerges as an alternative for topical application to unfavorable anatomical sites. This work highlights the potential of biomolecules to improve the wound remodeling phase through the modulation of type III and type I collagen deposition. The protective action of the carrier matrices was pivotal to sustain the activity of the biomolecules in the wound site. *In vivo* histological studies in spine epidural fibrosis are in progress to further investigate the role of PDGF-BB and PRP loaded with PA-6/SOMA in all phases of the wound healing and its integration with the host tissue.

Acknowledgments

The authors thank Mrs. Caroline Nesello for her vet technical support and Mrs. Raquel Brandalise and Mrs. Simone Andriolo Gross for their technical support in animal care at the University of Caxias do Sul. We recognize and thank the expert assistance of Dr. Luciano Selistre in statistics analysis.

Conflict of Interest Statement

The authors have declared no conflicting interest.

Author Contributions Statement

A.R.I, N.F.N. and, A.F. designed the experiments, analyzed the data and wrote the manuscript; M.F contributed in *in vivo* experiments and histological analysis; F.T.G.D. and O.B supported and produced the membranes used and made a critical review of the manuscript.

Table 1. Measurements of wound area contraction, epidermal thickness and collagen type III and I deposition.

Group	Wound Contraction (cm^2 ± SD)			Epidermal Thickness (µm ±SD)	*p (*)*	Collagen III (OD ± SD)	*p (*)*	Collagen I (OD ± SD)	*p (*)*
	Day 0	Day 14	(%)						
Control	0.983 ± 0.06	0,043 ± 0.007	95.9	83.71 ± 54.14	ref.	128594.28 ± 13155.05	ref.	64132.17 ± 30594.86	ref.
PDGF-BB	0.857 ± 0.031	0.032 ± 0.003	96.2	106.32 ± 30.08	1.00	113938.06 ± 37347.56	1.00	67298.89 ± 34439.19	1.00
PRP	1.080 ± 0.086	0.026 ± 0.003	97.5	108.11 ± 26.30	1.00	78460.39 ± 29341.07	0.003 (*)	26434.11 ± 14417.77	0.17
PA-6/SOMA	0.991 ± 0.071	0.060 ± 0.010	93.6	121.91 ± 27.82	1.00	107178.44 ±29728.79	1.00	48067.50 ± 22569.19	1.00
PA-6/SOMA + PDGF-BB	1.034 ± 0.090	0.029 ± 0.004	97.3	109.18 ± 66.52	1.00	72086.56 ±21666.83	< 0.001 (*)	49217.39 ± 9169.89	1.00
PA-6/SOMA + PRP	0.960 ±0.043	0.075 ±0.020	92.1	107.39 ± 36.95	1.00	97463.61 ± 32744.78	0.67	50767.94 ±27534.09	1.00

OD: Optical density; **PA-6/SOMA**: maleinized soybean modified polyamide-6; **PDGF-BB**: platelet derived growth factor-BB; **PRP**: platelet-rich plasm. The measurements of wound area contraction rate (C) was calculated based on day zero (A0; postoperative) and the reduction area rate obtained on the day 14 (A14), calculated by the following expression: C = A0 - A14. The rate of cicatricial contraction (TC) was obtained from the previous results by means of TC = C x 100 / A0. P < 0.05 (*): comparison to the respective control. Data were presented as means ± Standard Deviation (SD).

Figure Captions:

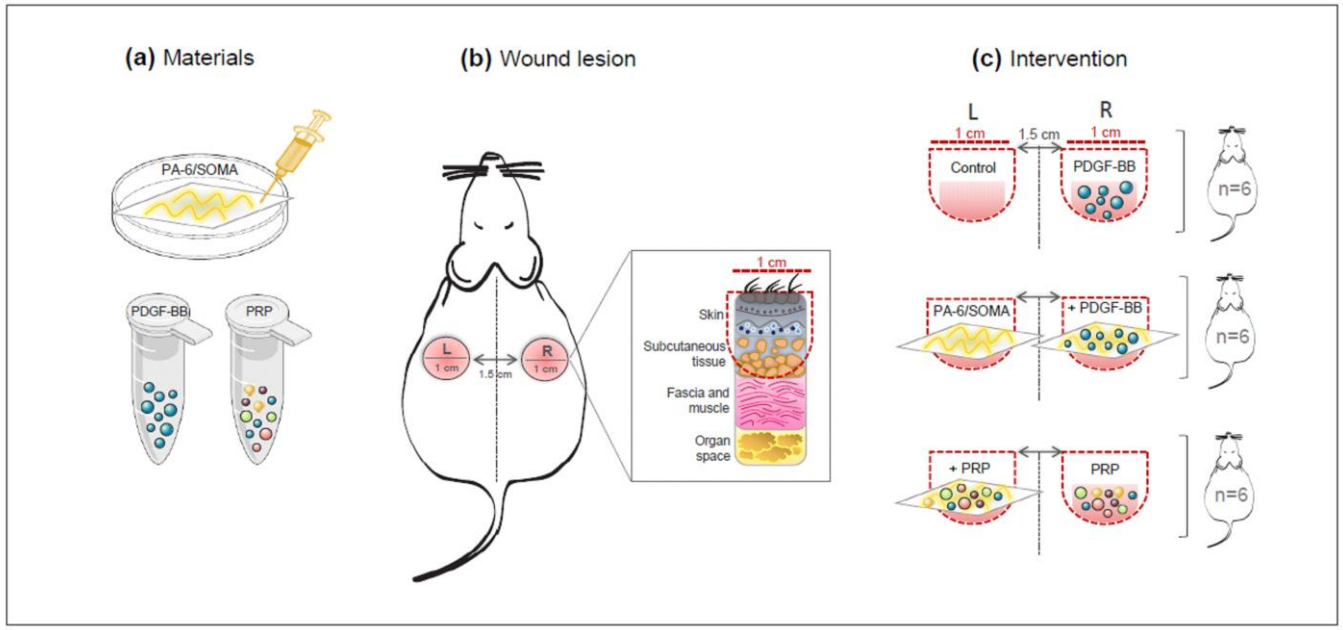

Figure 1. **Schematic study design of the experimental groups submitted to full-thickness in vivo wound model.** (a) Materials applied on the wound site. PA-6/SOMA, maleinized soybean modified polyamide-6; PDGF-BB, platelet derived growth factor-BB and PRP, platelet-rich plasm. (b) Wound lesion based on full-thickness wound when each animal was subjected to two incisional circular cutaneous resections, 1 cm in diameter using a cutaneous punch until the dorsal muscular fascia was exposed. (c) Animals were randomly divided into the following experimental groups (N = 6 per group): The control/PFGF-BB group received no application to the left lesion (L) and received application of growth factor PDGF-BB only to the right lesion (R). In the PA-6/SOMA + PDGF-BB group, the biomaterial enriched with maleinized soybean oil was applied to lesion left (L) and the same biomaterial loaded with PDGF-BB to lesion right (R). The PA-6/SOMA + PRP group received PRP in lesion left (L) and biomaterial PA-6/SOMA plus PRP in lesion right (R).

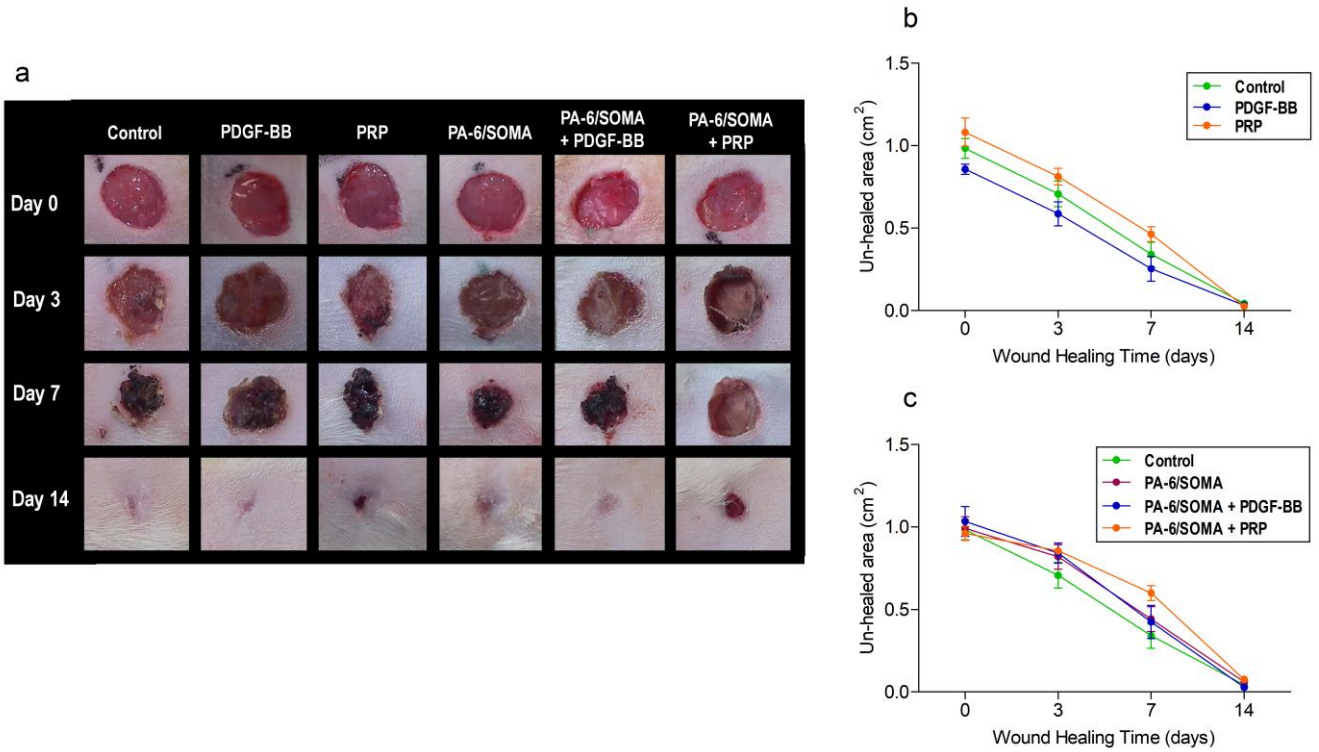

Figure 2. Time course of wound healing. (a) Representative pictures of wound lesions at different stages of the wound healing process at 0, 3, 7 and 14 days. (b-c) The points represent the average wound size (n = 6 animals) over the days of the experiment for each treatment regimen. Data were presented as means ± SD (n = 6) and the morphometric analysis between the groups during the observation period was determined by ANOVA with Tukey's post hoc test. PA-6/SOMA, maleinized soybean modified polyamide-6; PDGF-BB, platelet derived growth factor-BB and PRP, platelet-rich plasm

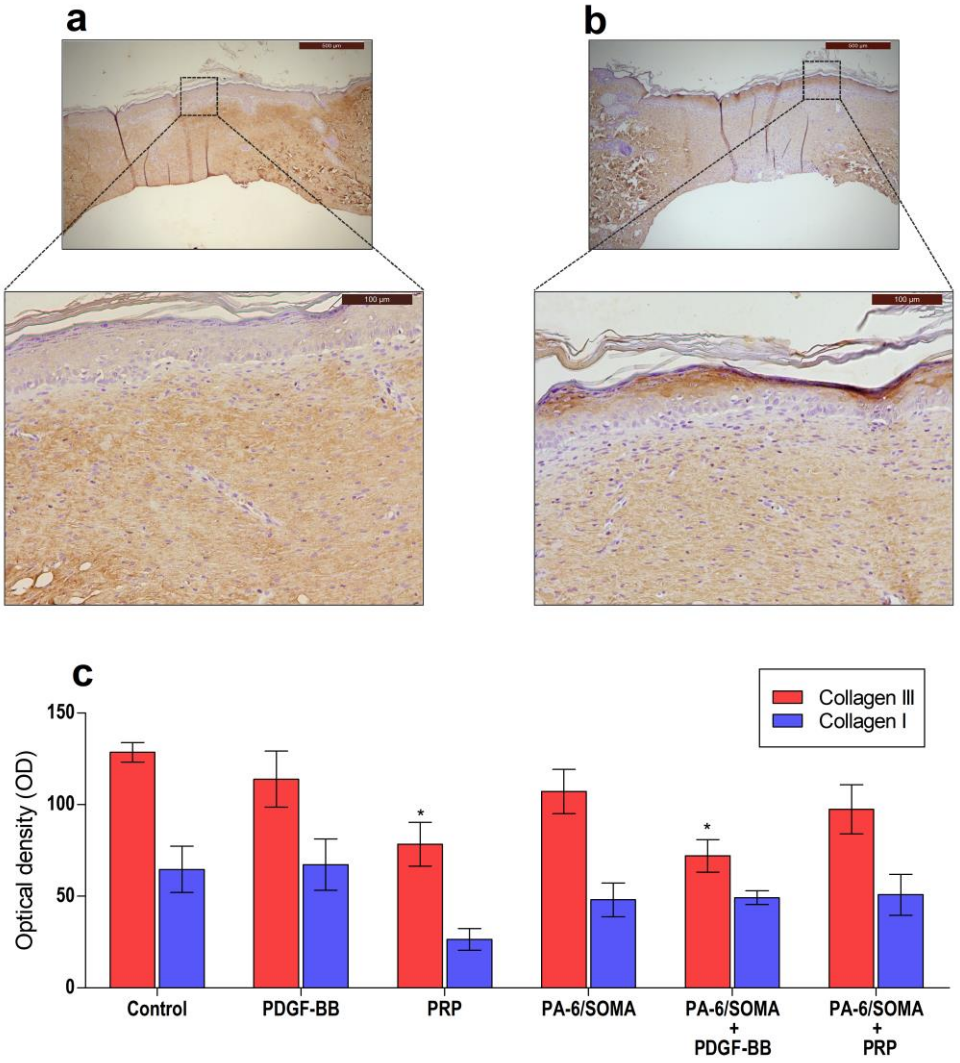

Figure 3. Immunohistochemistry analysis on the type III and type I collagen deposition. (a-b) Representative images of immunohistochemistry analysis for type III and type I collagen density in paraffin-embedded tissues. Scale bar = 50 μm; 100 μm. **(c)** Quantification of type III and type I collagen deposition by Image J software. Each column represents the mean ± SD (n = 6). *p < 0.05 for comparison *versus* control group determined by ANOVA. PA-6/SOMA, maleinized soybean modified polyamide-6; PDGF-BB, platelet derived growth factor-BB and PRP, platelet-rich plasm.

Supplementary files

Towards on the mediators in Collagen Replacement: effect of the active molecules into a Polymeric Biomaterial

Anderson Ricardo Ingracio[1], Natália Fontana Nicoletti[2], Fernanda Trindade Gonzalez Dias[3], Manuela Figueiró[2], Otávio Bianchi[1,3], Asdrubal Falavigna[1,2]

[1] Health Sciences Graduate Program, Universidade de Caxias do Sul (UCS), Caxias do Sul, RS, Brazil
[2] Cell Therapy Laboratory (LATEC), Universidade de Caxias do Sul (UCS), Caxias do Sul, RS, Brazil
[3] Materials Science Graduate Program (PGMAT), Universidade de Caxias do Sul (UCS), Caxias do Sul, RS, Brazil

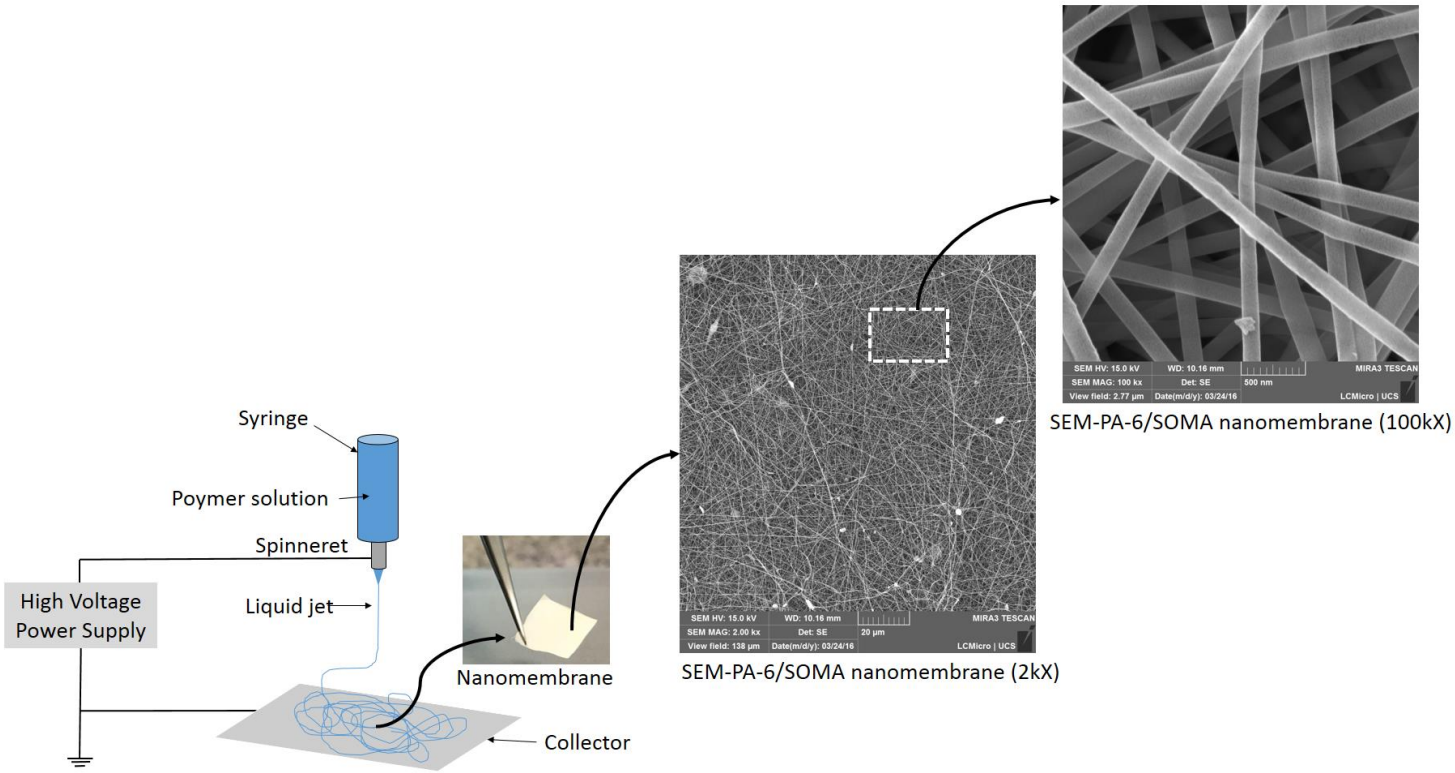

Figure S1. Scheme for nanomembrane production and SEM analysis

5. References

[1] T. Velnar, T. Bailey, V. Smrkolj, J Int Med Res. 2009, 37, 1528.
[2] J. E. Janis, B. Harrison, Plast Reconstr Surg. 2014, 138, 9s-17s.
[3] A. C. Gonzalez, T. F. Costa, Z. A. Andrade, A. R. Medrado, An Bras Dermatol. 2016, 91, 614.
[4] J. M. Reinke, H. E. Sorg, European Surgical Research. 2012, 49, 35.
[5] R. F. Diegelmann, M. C. Evans, Front Biosci. 2004, 9, 283.
[6] C. L. Baum, C. J. Arpey, Dermatol Surg. 2005, 31, 674.
[7] D. C. Rockey, P. D. Bell, J. A. Hill, N Engl J Med. 2015, 372, 1138.
[8] S. Sae-Jung, K. Jirarattanaphochai, C. Sumananont, K. Wittayapairoj, K. Sukhonthamarn, Asian Spine J. 2015, 9, 587.
[9] H. A. Bosscher, J. E. Heavner, Pain Pract. 2010, 10, 18.
[10] H. Erdogan, B. Kelten, M. Tuncdemir, S. P. Erturkuner, H. Uzun, A. Karaoglan, Neurol Neurochir Pol. 2016, 50, 323.
[11] E. Anitua, I. Andia, B. Ardanza, P. Nurden, A. T. Nurden, Thromb Haemost. 2004, 91, 4.
[12] A. T. Nurden, P. Nurden, M. Sanchez, I. Andia, E. Anitua, Front Biosci. 2008, 13, 3532.
[13] J. Alsousou, M. Thompson, P. Hulley, A. Noble, K. Willett, J Bone Joint Surg Br. 2009, 91, 987.
[14] M. F. Maitz, Biosurface and Biotribology. 2015, 1, 16.
[15] J. R. Ernzen, F. Bondan, C. Luvison, C. H. Wanke, J. D. N. Martins, Fiorio R, J Appl Polym Sci. 2016, 133, 10.
[16] F.T.G. Dias, N. F. Nicoletti, D. R. Marinowic, A. Ingracio, J. Catafesta, J. C. Da Costa, J.C, A. Falavigna, O. Bianchi, O. Annals of the 14th Brazilian Congress of Polymers. 2017, 1311-1317.
[17] M. Peletti-Figueiró, I. Silveira de Aguiar, S. Paesi, D. C. Machado, S. Echeverrigaray, M. Roesch-Ely1, A. Falavigna, J. A. P. Henriques. Columna/Columna. 2017, 16, 43.
[18] P. P. Bonvallet , M. J. Schultz , E. H. Mitchell, J. L. Bain , B. K. Culpepper , S. J. Thomas , S. L. Bellis, Plos One. 2015, 10.
[19] K. T. Kurpinski, J. T. Stephenson, R. R. Janairo, H. Lee, S. Li, Biomaterials. 2010, 31, 3536.
[20] A. Zonari, T. M. Martins, A. C. Paula, J. N. Boeloni, S. Novikoff, A. P, Marques, V. M, Correlo, R. L. Reis, A. M. Goes, Acta Biomater. 2015, 17, 170.
[21] P. P. Bonvallet, B. K. Culpepper, J. L. Bain, M. J. Schultz, S. J. Thomas, S. L. Bellis, Tissue Eng Part A. 2014, 17-18, 434.
[22] S. B. Mahjour, X. Fu, X. Yang, J. Fong, F. Sefat, H. Wang. Burns. 2015, 41, 1764.
[23] C. J. Yeh, C. C. Chen, Y. L. Leu, M. W Lin, M. M. Chiu, S. H. Wang, Sci Rep. 2017, 7, 15599.
[24] H. M. Mori1, H. Kawanami, H. Kawahata, M. Aoki, BMC Complement Altern Med. 2016, 26, 114.
[25] R.C. Fang, R.D. Galiano, Biologics. 2008, 2, 12.
[26] R. E. Marx, Implant dentistry. 2001, 10, 225.
[27] Dhurat R, Sukesh M, J Cutan Aesthet Surg. 2014;7(4):189-97.
[28] I. Mensik, E.N. Lamme, J. Riesle, Cell and Tissue Banking. 2002, 3, 245.

[29] P. Martin, W. R. Teodoro, A. P. Velosa, J. Morais, S. Carrasco, R. B. Christmann, Autoimmun Rev. 2012, 11, 827.
[30] P. Kuppan, K. S. Vasanthan, D. Sundaramurthi, U. M. Krishnan, S. Sethuraman, Biomacromolecules. 2011, 12, 3156.
[31] M. J. Barnes, L. F. Morton, R. C. Bennett, A. Bailey, T. J. Sims, Biochem. J. 1976, 157, 263.

[32] M. M. Al-Qattan, M. M. Abd-Elwahed, K. Hawary, M. M. Arafah, M. K. Shier. Biomed Res Int. 2015, 2015, 958695.
[33] H. J. Lai, C. H. Kuan, H. C. Wu, J. C. Tsai, T. M. Chen, D. J. Hsieh, T. W. Wang , Acta Biomater. 2014, 10, 4156.
[34] R. Vasita, I. K. Shanmugam, D. S. Katt, Curr Top Med Chem. 2008, 8, 341.
[35] R. Ravichandran, S. Sundarrajan, J. R. Venugopal, S. Mukherjee, S. Ramakrishna, Macromol Biosci. 2012, 12, 286.
[36] N. A. Smyth, C. D. Murawski, L.A. Fortier, B. J. Cole, J. G. Kennedy, Arthroscopy. 2013, 29, 1399.
[37] E. Anitua, M. Sanchez, G. Orive, Adv Drug Deliv Rev. 2010, 62, 741.
[38] E. Anitua, R. Tejero, M. M. Zalduendo, G. Orive, J Periodontol. 2013, 84, 1180.
[39] E. Anitua, A. Pino, G. Orive G, J Wound Care. 2016, 25, 680.
[40]. M. Sanchez, E. Anitua, D. Delgado, P. Sanchez, R. Prado, G. Orive G, Expert Opin Biol Ther. 2017, 17, 197.

4 CONSIDERAÇÕES FINAIS E PERSPECTIVAS

O PRP aplicado isoladamente exibiu uma menor concentração de colágeno tipo III. O momento em que foi realizado a biópsia, corresponde ao processo de remodelação tecidual com troca de colágenos tipo I pelo tipo III. O aumento dos níveis de colágeno tipo I ou mesmo a simples aceleração da lise de colágeno tipo III, podem refletir uma aceleração no processo de remodelação. Os mesmos resultados não foram obtidos pela aplicação do PRP associado à PA-6/SOMA. Isto pode refletir uma instabilidade decorrente da sua associação, contrária aos resultados obtidos *in vitro*, ou efeitos contrapostos e competitivos entre os mesmos. Ainda assim, o PRP foi promissor na modulação cicatricial, especialmente por sua riqueza nos diferentes FC e por constituir-se composto autólogo. FC utilizados de forma isolada, como PDGF-BB, são alternativas para a modulação cicatricial.

A fase mais adiantada da cicatrização é analisada dez dias após a lesão tecidual no rato. Neste período, existe uma reorganização da ME e troca de colágeno tipo III por colágeno tipo I. A PA-6/SOMA foi enriquecida por óleo de soja maleinizado devido ao seu efeito facilitador da epitelização. A modulação da deposição de colágeno tipo III e a presença da epitelização, foram os destaques positivos do uso da PA-6/SOMA. Vale salientar que, apesar da nanomembra PA-6/SOMA ter uma taxa de degradação lenta e não ser absorvida, não houve prejuízo no processo de epitelização.

É oportuno potencializar uma translação clínica utilizando a PA-6/SOMA em combinação com diferentes fármacos ou FC, uma vez que houve inibição da deposição de colágeno tipo III, aceleração no processo de remodelação e, no estudo *in vitro,* uma elevada proliferação celular e deposição de ME, sem vestígios de citotoxicidade. A propriedade de favorecimento à cicatrização, combinado com a propriedade de resistência tênsil e a característica de carreador de ativos biológicos, potencializa o uso do PA-6/SOMA como curativo em feridas ou como inibidor de fibrose excessiva.

O projeto de pesquisa proposto permite subsequentes estudos sobre a organização e orientação das fibras de colágeno e a sua influência na capacidade de resistência tensional e ao processo de gênese da fibrose. Somado a isto, a análise de propriedades fenotípicas mais específicas pode relacionar o processo de deposição de colágeno à força de tensão e resistência tecidual. Existe espaço também para análise da aplicação dos

fatores em tecidos orgânicos sadios, sem necessidade de reparo, em que não há influência da cascata fisiológica de cicatrização.

5 ANEXOS

5.1 Confirmação de submissão

Submission Confirmation

Print

Thank you for your submission

Submitted to
Experimental Dermatology

Manuscript ID
EXD-18-0226

Title
Towards on the Mediators in Collagen Replacement: Effect of the Active Molecules into a Polymeric Biomaterial

Authors
Ingracio, Anderson
Nicoletti, Natália
Dias, Fernanda
Figueró, Manuela
Bianchi, Otávio
Falavigna, Asdrubal

Date Submitted
11-Jun-2018

5.2 Artigo em colaboração submetido à publicação durante o Mestrado

Materials Science & Engineering C

POLYMERIC ELECTROSPUN MATS AS CUTANEOUS TOPICAL DRESSING FOR CHRONIC WOUNDS

Fernanda Trindade Gonzalez Dias[1]*, Anderson Ricardo Ingracio[2], Natália Fontana Nicoletti[3], Felipe Castro Menezes[4], Lucas Dall Agnol[2], Daniel Rodrigo Marinowic[5], Rosane Michele Duarte Soares[4], Jaderson Costa da Costa[5], Asdrubal Falavigna[2,3], Otávio Bianchi[1,2+]

1 – Materials Science Graduate Program (PGMAT), Universidade de Caxias do Sul (UCS), Caxias do Sul, RS, Brazil
*ftgdias@ucs.br, +otavio.bianchi@gmail.com

2 - Health Sciences Graduate Program, Universidade de Caxias do Sul (UCS), Caxias do Sul, RS, Brazil

3 – Cell Therapy Laboratory (LATEC), Universidade de Caxias do Sul (UCS), Caxias do Sul, RS, Brazil

4 – Poli-BIO, Polymeric Materials Research Group, Institute of Chemistry, Universidade Federal do Rio Grande do Sul
5 – Brain Institute of Rio Grande do Sul (BraIns), Pontifícia Universidade Católica do Rio Grande do Sul (PUCRS), Porto Alegre, RS, Brazil

Short running title: Polymeric topical dressing for chronic wounds

Summary

Engineered skin products have been adopted clinically, such as epidermis and dermis substitutes, and composite allografts. Nonetheless, these biomaterials demand intensive labor and an expensive final cost. In comparison to conventional bandages, which do not meet all the requirements of wound care, electrospun fiber mats could potentially provide an excellent environment for healing. In this work, we developed two nanostructured scaffolds based on polyamide-6 (PA-6) to be tested as a wound dressing in a rat model of full thickness incisional wound healing. The idea was to create a bioconstruct that is simple to implement and biologically safe, with a high survival rate, which provides physical support and biological recognition for new functional tissues. An unmodified PA-6 and a maleinized soybean modified PA-6 were employed as nanofibrillar matrices in this study. The biomaterials showed a dimensional homology

to natural extracellular matrix components and neither*in vitro* nor *in vivo* side effects. The PA-6 scaffolds were resistant to the sterilization process and could promote the attachment of 3T3 fibroblast and VERO cells, besides the incorporation of biological molecules. The modification of PA-6 chains with a fatty acid derivative increased the scaffold's surface free energy, favoring cell proliferation, collagen formation, and ECM secretion. These results show the potential of these materials as a topical dermal carrier for skin regeneration.

Keywords: *wound healing, polyamide-6, nanomembrane, electrospinning, cytotoxicity, growth factor*

1. Introduction

In the last decade, new technologies in wound dressings have been developed to improve healing in damage or loss of skin integrity. The cost to manage these wounds is likely to increase by $33 billion over the next ten years. Deep or chronic skin wounds arise in a great variety of pathological conditions including diabetic ulcers, arterial or venous disease, third-degree burn or as a result of irradiation for tumor treatment (Pal *et al.*, 2017). Skin wounds that do not regenerate in a timely and orderly fashion through the natural healing stages are considered chronic. The difficulty to heal spontaneously could be due to the lack of support to guide cell growth and reduced levels of endogenous growth factors (Yang*et al*., 2012). Patients with these conditions cannot endure procedures involving a large extent of skin surface, and their treatment relies on simple surgical dressing to regenerate wound areas. Topical wound management arises in this scenario to alleviate the patient's physical symptoms (such as exudate, malodor, pain, and bleeding) and also improve their quality of life.

Engineered skin products have been adopted clinically, such as epidermis and dermis substitutes, and composite allografts. However, current skin grafts still are labor intensive andhave a high final cost. In comparison to conventional bandages, which do not meet all the requirements of wound care, electrospun fiber mats could potentially provide an excellent environment for healing (Rieger, Birch and Schiffman, 2013). Nonwoven membranes have three-dimensional interconnected pore networks and a high surface area (Liu *et al*., 2017). Also, these materials are structurally similar to the extracellular matrices (ECM) in biological tissue, which is ideal for cellular attachment and proliferation (Unnithan *et al*., 2012). The electrospinning process can further be invoked to impregnate the nanomembranes with antibacterial and biological agents, thus improving cell compliance, and tissue regeneration (Rieger, Birch and Schiffman, 2013). Wound dressing materials produced by electrospinning also promise conformability to the wound contour and a scar-free healing process, two hard-to-find features in commercial adhesives.Biobrane and Mepitel, two examples of polyamide silicon membranes, are commercially used as synthetic skin substitutes, despite being expensive and difficult to manipulate and apply.

The use of polyamide based dressings in the management of burns have been reported in the literature (Cai *et al*., 2014). Nylon can be engineered to degrade at a slow rate while having a minimal negative impact on the surrounding tissues. Besides, electrospun nylon nanofibers can offer a hydrophilic surface, good mechanical strength, and suitable biocompatibility as ideal properties for skin wound healing (Garcia-Orue *et al*., 2017; Liu *et al*., 2017). For chronic

injuries, it is desirable to cover the wound with an adherent dressing which will control skin homeostasis, loss of body water and prevent infection. In this particular case, the dressing should slowly degrade and allow the tissue to grow into the nanofibrous material interstices, being assimilated by the body and acting as an ECM.It must have a long shelf life and be durable with long-term wound stability. Designing prolonged-action scaffolds that are resorbable and do not degrade in the body releasing toxic metabolites is an important objective of biomedical research (Rieger, Birch and Schiffman, 2013).

Polyamides are structurally similar to proteins, and theirbreakage can produce free amine and carboxylic acid derivatives. The hydrolytic degradation of a polyamide-6 (PA-6) based implant under physiological conditions (pH ~ 7.0 and 37 ºC) starts by the second week after intervention, and 15-20% is degraded per year (Marqués *et al*., 2000). In contrast, poly(lactic acid) (PLA), a commonly chosen biodegradable polymer for dressings, loses 75% of its weight in less than 40 days when immersed in buffer solutions.In the case of polyamides, the mat degradation rate can be tunable, respecting the patient's needs (Rieger, Birch and Schiffman, 2013).

In this work, we developed two electrospun scaffolds based on PA-6 to be investigated as an *in vivo* sacrificial substrate for the epithelialization of wounds.The idea was to create a bioconstruct that is simple to implement and biologically safe, with a high survival rate and that provides physical support and biological recognition for the new tissue formation. An unmodified PA-6 and a maleinized soybean modified PA-6 (PA-6/SOMA) were employed as nanofibrillar matrices in this study. The soybean oil presented in SOMA has a source of essential fatty acids and tocopherols,related to antioxidant and anti-inflammatory and epithelizing properties. We hypothesized that wound dressings containing SOMA might contribute to a more natural healing process and be a suitable adjuvant to currently available treatments for chronic cutaneous wounds. Besides, the incorporation of SOMA to PA-6 chains also imparts toughness to thepolymer, which is necessary for support handling and cellular morphogenesis. This article focuses on the structural properties of biomaterials developed and, also on the effect of PA-6 chemical modification in cytotoxicity and biomolecule affinity. Furthermore, the nanofibrous mats behavior when in contact with the wound microenvironment was preliminarily investigated.

2. Materials and Methods

2.1. Materials

PA-6 resin (RADILON S40F) (M_v: 53,000 $gmol^{-1}$) was donated by “Mantova Industria de tubos flexíveis” (Caxias do Sul, Brazil). The PA-6/SOMA (M_v: 66,000 $gmol^{-1}$) sample was produced by the reaction of PA-6 chains with 5%wt. of maleinized soybean oil (SOMA) in a co-rotating twin-screw extruder (Ernzen *et al*., 2016). Formic acid 85% v/v purchased from Neon Comercial (São Paulo, Brazil) was used as a solvent without further purification. VERO (kidney epithelial cells of African green monkey) and 3T3 (murine fibroblast) cell lines were from American Type Culture Collection (ATCC-Rockville, Maryland, USA). The recombinant human platelet-derived growth factor (rhPDGF-BB) was purchased from Pepro Tech Inc. (Rocky Hill, NJ).

2.2.Nanomembrane production and characterization

The nanofibrous mats were prepared by an electrospinning apparatus (INSTOR, Porto Alegre, RS) from solutions of PA-6 and PA-6/SOMA in formic acid. Different electrospinning conditions and concentrations of polymeric solutions were tested on fiber production (see in supplementary files, Table S1). Defect-free membranes were obtained from 32%wt. solutions at a feeding rate of 0.1 ml/h, using a syringe-collector distance of 15 cm and an applied voltage of 25 kV. The electrospinning process was carried out at room temperature. ATR-FTIR analyses were used to verify the presence of residual formic acid by the 1727 cm^{-1}band and no solvent trace was found in the fibrous mats (result not shown). The nanofiber morphology wasevaluatedby field-emission scanning electron microscope Mira 3 Tescan (FEG-SEM) (Czech Republic). Samples were coated with gold using a plasma sputtering apparatus for FEG-SEM analysis.For each sample, at least 50 fibers were manually measured and analyzed using ImageJ software (NIH, USA). The average fiber diameters were expressed asmean standard deviation.

The Wide-Angle X-ray Diffraction (WAXD) pattern of the electrospun mats was investigated to obtain information about the microstructure of materials. The analyses were performed at 20ºC using a Shimadzu XRD-6000 diffractometer. Scans were carried out from 3º to 40º (2θ) at a scan rate of 2º/min using Cu-Kα radiation. The diffractograms were mathematically treated to estimate the relative fractional crystallinity and the amount of γ-form polyamide crystals. The structure of the materials was evaluated using small-Angle X-ray Scattering (SAXS) experiments. The experiments were performed on the SAXS1 beamline of the Brazilian Synchrotron Light Laboratory (LNLS), usinga Pilatus detector (300k Dectris) positioned at 836 mm and scattering wave vectors (q) from 0.13 to 2.5 nm^{-1}. The wavelength (λ) of the incident X-ray beam was 0.155 nm.

The surface free energy of the PA-6 and PA-6/SOMA samples was determined by the Owens–Wendt method, which is based on contact angle measurements conducted with certain measuring liquids (Stachewicz and Barber, 2011). Although it cannot be assumed that the surface properties of electrospun mats are similar to those of bulk, the wett ability behavior of the pristine solid specimens will already allow us to predict the hydrophilicity of these nanomembranes. The contact angle measurements were carried out in an SEO® Phoenix100 (Korea) equipment and fiveprobe liquids were employed: distilled water (γ_L^P = 51.0 mJ/m^2; γ_L^D = 21.8 mJ/m^2; γ_L = 72.8 mJ/m^2), glycerin (γ_L^P = 29.7 mJ/m^2; γ_L^D = 33.6 mJ/m^2; γ_L = 63.3 mJ/m^2), dimethyl sulfoxide (γ_L^P = 8.0 mJ/m^2; γ_L^D = 36.0 mJ/m^2; γ_L = 44.0 mJ/m^2), n-hexadecane (γ_L^P = 0.0 mJ/m^2; γ_L^D = 27.6 mJ/m^2; γ_L = 27.6 mJ/m^2) and bovine serum albumin (BSA) aqueous solution (1 g/dl) (γ_L^P = 2.5 mJ/m^2; γ_L^D = 38.3 mJ/m^2; γ_L = 40.8 mJ/m^2); where γ_L^P, γ_L^D and γ_L represent the polar component, the dispersive component and the surface free energy of the liquids, respectively. The sessile drop method was adopted using 2 μL drops. The contact angle was measured at least ten times at different sites on the surface, the average value being considered.

2.3.PA-6 nanomembranes as wound healing materials

2.3.1. Affinity with biomolecules

To evaluate the attachment of peptides to the nanofibrillar surfaces, PDGF-BB was used. The growth factor (GF) was reconstituted in 0.1wt.% BSA and diluted with ultra-pure water to achieve a concentration of 10 μg/mL and stored

at -80ºC. PDGF-BB (100 ng/mL) in solution was added to PA-6 and PA-6/SOMA nanomembrane surfaces and incubated for 45 minutes at 37ºC. The GF attachment to the membrane was examined by ATR-FTIR and FEG-SEM.

2.3.2. *In vitro* cytotoxicity and cellular adhesion

VERO and 3T3 cells were cultured in Dulbecco's Modified Eagle Medium with 10wt.% fetal bovine serum (FBS) at a temperature of 37 °C, a minimum relative humidity of 95%, and an atmosphere of 5wt.% CO_2 in air. PA-6 nanofibrous mats (N=3 per group per experiment) were sterilized under 120 mmHg pressure for 45 minutes and subsequently dried at 37ºC for seven days. The cell lines were incubated with commercial PA-6 and PA-6/SOMA nanomembranes by direct contact and elution methods at a size corresponding to 3 cm^2/mL, as recommended by ISO 10993 (2009)(ISO 10993-5, 2009). All experiments were performed three times in triplicate. To assess cell viability, the metabolically active mitochondria were evaluated by MTT assayat 24 h, 48 h, and 72 h. To verify cell adhesion, the materials were held in the deep 24-well plate and the cells were seeded on the membranes at the density of 15-20×10^3 cells per well,and cultured for 24 h or 72 h. The cells were fixed with 2.5vol.% glutaraldehyde, and sequentially dehydrated in increasing concentrations of ethanol (50, 70, 85, 95 and 100vol.%). The samples were left for 1 h in 100% ethanol and allowed to air dry at room temperature. Cell morphology and adhesion were assessed by SEM results.

2.3.3. *In vivo* wound healing evaluation

Wistar albino male adult rats (8 weeks old, 250–300 g; total N= 37) were used to evaluate the *in vivo* dressing by a wound healing model. The animals were housed under conditions of optimum light, temperature and humidity (12 h light-dark cycle, 22±1°C, under 60 to 80 % humidity), with food and water provided *ad libitum*. The animals were supplied by the Federal University of Rio Grande do Sul (UFRGS, Brazil). All the experimental procedures were in accordancewith the Principles of Laboratory Animal Care from NIH, and were approved by the local Animal Ethical Committee (CEUA-UCS; protocol number: 015/2016).

Two incisional full-thickness circular wounds (1 cm in diameter) were made on the upper back of each animal using a sterile punch. The animals were previously anesthetized by an intraperitoneal administration of ketamine and xylazine (80 and 10 mg/kg, respectively). Equal areas of the wound sizes were treated with either control (untreated wound) or commercial PA-6 or PA-6/SOMA (loaded with GF or not) membranes placed inside the wound, not sutured to the skin (N = 6 animals/group; Total N = 36). After recovery from anesthesia, the animals were placed in individual cages, and the wound sites were observed macroscopically throughout 14 days. An animal (N = 1) was used to evaluate the nanofibrillar surface of PA-6/SOMA (loaded with GF or not) after 3 days within the wound. Microscopic evaluation of cell content on the nanofibrillar surface was made by FEG-SEM.

2.3.4. Statistical analysis

The number of experimental replications is provided in the Figure legends. Data from *in vitro* experiments were analyzed by one-way analysis of variance (ANOVA) followed by Bonferroni's post-hoc test, using Graph-Pad Software (San Diego, CA, U.S.A.). $P<0.05$ was indicative of statistical significance.

3. Results and Discussion

3.1. Morphological and structural properties of nylon-6 nanomembranes

Figure 1 shows the morphological appearance of the produced electrospun scaffolds. The processing parameters influenced fiber formation during electrospinning, among which viscosity of the polymeric solution was vital to spinnability and fiber morphology (Chen *et al*., 2016). The PA-6 and PA-6/SOMA fibrous mats (Figure 1a and b) were composed of uniform, random and free-globular fibers and exhibited average diameters of 171.0 ± 11.0 nm and 250.0 ± 9.0 nm, respectively. The PA-6/SOMA slightly increased the average diameter of the fibers, mainly due to the molecular weight of the modified polymer (Unnithan *et al*., 2012). Interestingly, these diameter values are within range of extracellular matrix collagen fibers (ECM) (50 – 500 nm) (Garcia-Orue *et al*., 2017). This is a good starting point toward the development of a synthetic scaffold able to reproduce the natural structure of ECM. Besides, a sterile dressing is necessary to prevent wound contamination and subsequent infection (Cai *et al*., 2014). In this regard, these nanomembranes were able to withstand an autoclave sterilization process (120 mmHg/45 min), showing that the aseptic process did not affect the structural integrity of PA-6 nor the average diameter of the fibers (Figure 1c and d).

The effect of polymer processing and its effect on structural conformation is essential to understand the material property. For example, changes in the structure of the crystal phase and the crystal size might directly impact on the physicomechanical characteristics of polymers as well as theirbiological response (Richard-Lacroix and Pellerin, 2013;Stephens, Chase and Rabolt, 2004). Not only the chemical architecture of the fiber is important, but its ability to form a 3D network which promotes cellular activity. In this context, the electrospinning process effect on nylon-6 chain conformation and crystal structure should be investigated. The WAXD analysis elucidates the structure/property/process relationships in electrospinning, making it possible to understand the microstructure developed during fiber formation. PA-6 is a polymorphic material, having more than one energetically favorable crystalline phase such as α and γ-forms (Richard-Lacroix and Pellerin, 2013. The α form of PA-6 usually exhibits two characteristic reflections around 20.3º and 23.8° (2θ) whereas the γ form presents a distinctive reflection at 21.6º (2θ) (Tsou, Lin and Wang, 2011). The three crystalline phases were clearly detected in the pre-electrospun PA-6/SOMA diffractogram (see supplementary data, Figure S1) (Ernzen *et al*., 2016). For the other samples, the diffraction patterns revealed a single peak at about 21º (2θ). Little is known about the crystalline structures and their transitions in PA-6 electrospun nanofibers. For this polymer, the free energies of the α andγ-forms are relatively close to each other, which allows the interconversion between these forms upon the use of certain solvents or experimental conditions (Stephens, Chase and Rabolt, 2004).

Quantitatively, peak deconvolution was used to estimate the fractional crystallinity and the amount of γ-form crystals (see supplementary data, Table S2). The relatively amorphous and crystalline phases were computed according to the procedure developed by Brian P. Grady(a software written in Excel available on his website), which fits the crystalline

peaks and amorphous halo through a Gaussian–Lorentzian area function. The results indicated that the electrospinning process led to a crystallinity reduction when compared to the solid samples. This can be justified by the high stress applied during fiber formation in the electrospinning process, which does not allow for the necessary time for crystallization to develop (Richard-Lacroix and Pellerin, 2013; Stephens, Chase and Rabolt, 2004). The amount of γ-phase also decreased from the solid samples to the electrospun fibers. The development of γ-form crystals in as-spun fibers occurs preferably in solutions with low polymer contents (4 - 12 wt.%) whereas, at higher concentrations (as in our case), this phase content is gradually reduced (Tsou, Lin and Wang, 2011). Since there is a substantial overlap between the positions of the amorphous and crystalline peaks, the fitted parameters should only be used to compare the samples within this experiment in qualitative trends.

PA-6 and PA-6/SOMA materials showed a typical I(q) vs. $q^{-3.7}$in SAXScurves (see supplementary files, Figure S2), which it is characteristic of fibrillar structures elongated in one direction (Gazzano *et al*., 2015; Richard-Lacroix and Pellerin, 2013; Stachewicz and Barber, 2011). The nanomembranes showed a reduction in the long lamellar period from ~10 nm to 5.7 nm, due to the orientation of polymer chains during the electrospinning process. The elongation force during the electrospinning process dramatically influences the macromolecular assemblies within the fibers, in particular their macromolecular orientation, chain conformation, and crystal structure. The nonwoven electrospun mats revealed isotropic strong diffuse scattering near the beam stop, which can be attributed to nanofibrils or microvoids within these nanostructures. The 2D SAXS patterns for the electrospun scaffolds exhibited a circumferential shape representing the lack of structural alignment along the fiber axis as well as the scattering from fibers in all directions (Gazzano *et al*., 2015).

For biomaterials applications, the adhesion phenomenon plays a significant role.Thus the surface free energy must be investigated through its dispersive and polar components. The biological molecules affinity for a 3D scaffold is profoundly affected by the nature of the biomaterial surface (Stachewicz and Barber, 2011). Increased nanomembrane wettability also improves implant tissue integration (Abdal-hay,Tijing and Lim, 2013). The Owens-Wendt theory determines the polar and dispersive contributions to a solid's surface free energy using the known polar and dispersive components of the probe liquids and their contact angles with the solid (see supplementary data, Table S3) (Stachewicz and Barber, 2011). The total surface free energy of the PA-6 solid sample was 47.5 mN/m, which is in agreement with the literature values (Pal *et al*., 2017; Stachewicz and Barber, 2011). The PA-6/SOMA has contributed to the increase of surface free energy, which favors adhesiveness energetically and might help obtain a cell response. The higher the surface free energy value the higher the wett ability and bioactivity of a biomaterial. From the contact angle results with n-hexadecane, it is clear that the chemical modification has made PA-6/SOMA material moderately hydrophilic. Many studies have demonstrated that cells adhere, spread and grow more easily on moderately hydrophilic substrates than on hydrophobic or very hydrophilic ones (Pal *et al*., 2017; Yang *et al*., 2012). The PA-6/SOMA sample also presented higher affinity with BSA solution, confirming a more pronounced interaction with the protein molecules. The association of long-chain fatty acids with BSA has a physiological significance since albumin is the principal vehicle for free fatty acid (FFA) transport through the plasma. The association of FFA with albumin is thought to involve electrostatic attraction of the FFA carboxyl group to protein cationic sites together with hydrophobic interactions between the FFA hydrocarbon tail and nonpolar side chains of the protein.

3.2. Nanomembrane interaction with the PDGF-BB growth factor

The development of bio-active matrices from scaffolds embedded with growth factors can provide the necessary biological recognition in the wound healing process (Chen *et al*., 2016). The affinity of a recombinant human PDGF-BB by the nanofibrillar surfaces was evaluated for the purpose of activating cell-material interactions. The nanofibrous scaffolds successfully loaded the chosen growth factor PDGF-BB. The incorporation of this biomolecule to the PA-6/SOMA nanomembrane was confirmed by FEG-SEM and FTIR results (Chen *et al*., 2016) (Figure 2). The PDGF-BB spectrum indicated the presence of an intense peak at 1641 cm^{-1} and a weak signal at 1549 cm^{-1}, both related to protein amide bands (Reigstad *et al.,* 2003). The PA-6/SOMA nanomembrane loaded with PDGF-BB demonstrated some characteristic bands that were absent in the pure PA-6/SOMA spectrum. This result shows the possible incorporation of growth factor onto electrospun nanofibers.

PDGF-BB is a diffusible signaling protein mediator, essential for a successful tissue repair throughout the three phases of wound healing. The pharmacological activity of rhPDGF-BB is similar to the naturally released PDGF and comprisesthe promotion of chemotactic recruitment, formation of granulation tissue and cell proliferation. The rhPDGF-BB gel (becaplermin) is the only currently approved growth factor therapy for the healing of diabetic neuropathic foot ulcers and non-healing wounds (Andrae, Gallini and Betsholtz, 2008).The tissue repair mechanisms induced by PDGF-BB appear to involve fibroblast proliferation, collagen production, and neovessel formation.

Clinical efficacy has been demonstrated in several phase III studies (Smiell *et al.*, 1999), and the combined results suggest that topical application of PDGF-BB is safe and well tolerated. The binding capability of growth factor interaction with scaffold is critical for preserving and achieving maximal bioactivity, which has been a relatively less emphasized issue in previous studies (Mammadov *et al*., 2012). One of the major obstacles is the peptides which are either quickly degraded by proteases or removed by proteases or removed by exudate before reaching the wound bed. Although numerous covalent immobilization strategies have been proposed, specificity of the coupling site on the growth factors is difficult to achieve, and proteins lose their functionality during the coupling process.

More interestingly, in this set of experiments, PA-6/SOMA nanofiber scaffolds can interact with the growth factor noncovalently, not requiring the use of covalent chemistry for the coupling process. This observation is correlated with thesurface free energy results (see in supplementary files, Table S3).Protein binding affinity to a biomaterial is determined by Coulomb forces and van der Waals interactions (Nur-E-Kamal *et al*., 2008), in this specific case, the amine groups of the polyamide and PDGF-BB can interact by hydrogen bonds. This reveals that polyamide nanofibers can effectively mimic the chemistry of extracellular matrix, being promising materials for regenerative medicine applications through efficient growth factor delivery.

3.3. Interaction of nanomembranes with the 3T3 and VERO cell cultures

The effects of PA-6 and PA-6/SOMA mats were initially evaluated by MTT assay in two distinct cell lines. No significant differences in cell biocompatibility were observed

betweencommercial PA-6 and PA-6/SOMA nanofibrous scaffolds, as shown in Figure 3. Neither nanomembrane displayed any cytotoxicity in fibroblast 3T3 and VERO lineages in up to 72 h, denoted that PA-6 and PA-6/SOMA cannot affect the favorable cell environment. Strikingly, insofar these materials induced a promising enhancement of cell viability at 48 h for fibroblast 3T3 lineage, the VERO cells, recommended for screening chemical toxicity *in vitro*, remained viable and able to spread and reproduce. These findings are compatible with the ability to grow and colonize the structure of the materials produced (Unnithan *et al*., 2012).

The cell adhesion affinity by PA-6 and PA-6/SOMA was investigated 24 h post-seeding 3T3 fibroblasts deposited onto the nanofibrillar surfaces (Figure 4). In the first 24 h of culture, the fibroblast showed a rounded morphology for both nanofibrous mats (4.2 μm; PA-6/SOMA), but adherent contact points with the surrounding fibers and release of ECM by cells could be seen mainly inthe PA-6/SOMA sample (Park *et al*., 2007). 3T3 cells cultured on PA-6/SOMA appeared healthy and exhibited a well-spread and elongated morphology (6.4 μm; PA-6/SOMA) in comparison with fibroblasts grown on PA-6, with extensive projections after 72 h, indicating favorable cell adhesion and migration toward the PA-6/SOMA nanomembrane (Abdal-hay, Tijing and Lim, 2013).

The cells spread over the fibers by cytoplasmic extensions. This morphology is consistent with a classical in vivo-like fibroblast phenotype (Schindler *et al*., 2005). The images show that the adhered cells stretched more easily and deposited more ECM across the random SOMA-containing scaffold, better than cells on the pristine PA-6 scaffolds. This behavior confirms the surface free energy results, which revealed an increased adhesiveness to the PA-6/SOMA surface (see in supplementary files, Table S3). The PA-6/SOMA scaffold structure accelerated the adhesion and the proliferation rates of 3T3 fibroblast cells. The greater percentage of cells that attached to SOMA-containing scaffold could be in part explained by the influence of the surface's polar character, which leads to an enhancement of fibroblast attachment (Yang *et al*., 2009).

Regarding distinct cell types driven by different cues, Lukyanova *et al*.(2010) reported that non-toxic compounds like soybean oil induce a microenvironment which favors osteoblastic cell migration. The proliferation of preosteoblastic cells on polymeric soybean oil-g-polystyrene membranes was enhanced by the increased soybean oil content (Aydin *et al*., 2013). The bioactivity of soybean-based biomaterials favored the osteoblast differentiation *in vitro* and bone repair *in vivo* in rabbit models (Santin and Ambrosio, 2008). Promising cells adhesion and growth were also observed in L-929 from mouse connective tissue when exposed to soybean oil-based polyurethane networks (Miao *et al*., 2012). On the other hand, an interesting research headed by Xie *et al*. (2014) suggested an antiproliferative effect in mouse keratinocytes through the use of soy-derived phosphatidylglycerol. This proposal opens new insights into the treatment of different skin diseases, characterized by excessive or insufficient proliferation.

Distinct PA6-blended scaffolds have been prepared and investigated to enhance the cytocompatibility of PA-6 to support treatments for a wide variety of pathologies. A biphasic scaffold composite of PVA/Gel/V-n-HA/PA6 was favorable to BMSCs integration and promoted osteochondral regeneration when applied *in situ* to an osteochondral defect (Li *et al*., 2015). Treating osteochondral defects is challenging since the interfacial tissue between bone and cartilage has different biological cues to regenerate. The manufactured bi-layered scaffold PVA/Gel/V-n-HA/PA6 supported disparate

abilities of the native osteochondral unit and fulfilled the requirements to integrate the newly formed osteochondral matrix with the surrounding tissues.Nanofiber scaffolds fabricated from PA6-12 have been used to hold growth and proliferation of different stem cells sources. Zajicova *et al.*(2010) chose such a copolymer as a matrix for the growth of corneal epithelial and endothelial cell lines. The PA6-12 scaffolds supplied the growth of adult-tissue specific cells and their transfer to treat ocular surface injuries.

Cytocompatibility properties of synthesized hybrid PA-6 blends were investigated using EA.hy926 human endothelial cells. PA-6 has been engineered to retain mechanical strength and durability in a tissue scaffold. Fibrous scaffolds prepared from different weight ratios of PA-6/PCL blends proved to be an excellent endothelial cell carrier and exhibited promising morphological features, relevant to peripheral blood vessel materials (Abdal-hay*et al*., 2017).

3.4. Interaction of nanomembranes with the in vivo wound microenvironment

The behavior of nanomembranes in direct contact with the wound microenvironment was assessed in the first 72 h after application. The PA-6 and PA-6/SOMA scaffolds were analyzed, wether or not loaded with PDGF-BB. The biomaterials remained fixed at the wound site the entire time, without the need of sutures to attach them in position. The ease of handling while the dressing was applied and the ability to adhere and conform to the wound surface were mechanical characteristics that were noteworthy (Cai *et al*., 2014). Wound dressings need an ideal structure: one that offers high porosity and provides a good barrier. Such mechanical properties suggest that the PA-6 and PA-6/SOMA nanofiber scaffold realistically mimics the mechanical characteristics of the soft tissue. The porous structure of electrospun fibrous mats could also absorb excess exudates (Yang *et al*., 2012).

The biomaterial surface removed from the wound bed after 72 h in direct contact was observed by FEG-SEM (Figure 5). The microscopic images revealed a more pronounced cellular proliferation, collagen fibrils formation and remarkable ECM secretion for the PA-6/SOMA loaded with PDGF-BB. The ECM confers resistance to the injured histological tissue (Janis and Harrison, 2014). Collagen fiber is the framework of the dermis, and a healing wound is mainly a result of the net deposition and stabilization of collagen in the wound area providing strength and protecting it from traumatic damage (Yang *et al*., 2012). Thus, collagen formation is a determinant event in the physiological healing process, causing pathological consequences when deficient deposition or alteration of the degradation rates are observed (Janis and Harrison, 2014). The presence of a variety of dermal cell phenotypes on nanofiber mats was detected on the 3rd postoperative day. Over time, the biomaterials should be populated by crucial factors and other connective-tissue cells typical of the healthy skin wound microenvironment. The signs of biological events were less expressive in the commercial PA-6 nanomembrane. Cells grown on the pristine PA-6 surface were not well-spread across the surface and grew as a non-continuous monolayer (Figure 5). In contrast, the cells seeded on the PA-6/SOMA samples had a dendritic appearance with extensions (Abdal-hay, Tijing and Lim, 2013).

As expected, PA-6/SOMA loaded with PDGF-BB performed best in attracting cells and intensified the proliferation rates of the different cell types that comprise the wound microenvironment, with more collagen content and ECM deposition (Figure 5). The PDGF-BB release might promote the endothelial growth and proliferation as its mitogenic effect. PDGF-BB is responsible for the differentiation of fibroblasts into their contractile phenotype, the

myofibroblasts, which play an active role in producing and maintaining the ECM, signaling through mechanical stress and providing response elements for the immune system. Several animal studies had demonstrated accelerated wound closure in normal and pathophysiological states when the wound bed was supplemented with exogenous PDGF (Uhl *et al*., 2003). The permeable background provides the essential humidity and probably offers the sustained release of the PDGF-BB, preventing drying of the wound site and supporting tissue repair. It is important to emphasize that these features also eliminate the continual wound redressing and cleaning requirement, helping the body to heal successfully and inhibiting the patients' distress at chronic wounds.

3.5. In vivo wound-healing assay: Macroscopic observation of the wound-healing process

The PA-6/SOMA nanomembranes have presented excellent biocompatibility with the wound microenvironment, dimensional homology to the natural components of ECM and adequate properties to promote the attachment of biomolecules and attract cell types present in the healing phases. At the time, the cutaneous lesion was also evaluated *in vivo* through 14 days post-wounding. The nanofibrous materials were biocompatible and did not cause any local inflammatory reaction in a macroscopic *in vivo* evaluation. Figure 6 shows the macroscopic observation of the cutaneous healing evolution after treatment with fibrous mats, using an untreated wound as the control. For all groups wounds were observed with serosanguineous crust formation adhered to the injury site after a certain time, including the groups treated with the biomaterials. The cells can secrete proteins that induce the creation of a fibrous capsule around the implanted biomaterial. The nanofiber mats behaved as an interfacial tissue, being encompassed by the fresh tissue formed. As new granulation tissue is being generated, the wound contracts (Rieger, Birch and Schiffman, 2013).

The wounds that did not receive the biomaterial treatment developed granulation tissue on the 3rd-day post procedure. Early granulation tissue formation also signified autolytic debridement of wound exudates, restricted tissue necrosis, and shortened inflammatory phase (Pal *et al*., 2017). However, no macroscopical differences were observed between the wound contraction rates for all groups at the specified times. The wound closure of the animals was not significantly accelerated by the nanofibrous scaffolds in both the absence and presence of growth factor within a 14-day follow-up. These results do not exclude the possibility that the nanomembranes are capable of modulating other healing parameters at the cellular level. Moreover, the physical strength generated by the biomaterial application on the wound site did not preclude the wound contraction, which denotes the possibility of PA-6/SOMA being applied as a dressing with the potential to carry active biomolecules topically.

The induction of collagen deposition on the wound site by these biomaterials already highlights their capability to repair tissue. It is possible that these biomaterials also act as a physical protection against infection. Even after 14 days of treatment, polymeric fibers did not degrade through the phagocytosis of cells and the invasion of tissue fluids (Pal *et al*., 2017).In time, the body breaks down the biomaterial and only a newly formed skin layer should remain. Five patients with different causes of burn injury were treated with a dermal scaffold based on PEGT/PBT copolymer (Mensik *et al*., 2002). In the same way as polyamide, this copolymer also slowly degrades. One-year post-treatment, intracellular fragments (size up to 100 μm) of the PEGT/PBT copolymer were observed by SEM, indicating that cells were able to phagocytize it. Fast degrading dermal biomaterials induce more acute inflammation, which in a wound could negatively affect the healing process. Moreover, if the scaffold degrades much faster, its mechanical stability and 3D structure are

quickly lost, as is, consequently, the support for tissue ingrowth. Masrouha *et al.* (2016) firstly reported the epithelialization of the skin over a polymeric scaffold in three illustrative cases of patients. The polymeric scaffold provided a surface for epithelial regeneration and secondary wound closure. In a six-week period, the wound shrank with healthy granulation tissue covering the implanted material, followed by epithelialization and complete closure of the defect with no discharge. At 5-year follow-up, the patients were fully ambulatorial with no clinical signs of infection.

The use of Biobrane and Mepitel polyamide dressings in the management of wound injuries is well-known in the literature (Cai *et al*., 2014; White and Morris, 2009). Unfortunately, these adhesives are expensive and have low conformation over concave surfaces, besides being adherent to gloves and surgical instruments. Biobrane and Mepitel could be improved by increasing their flexibility, a limitation that has motivated the development of the electrospun PA-6 scaffolds. Despite the recent advances in cell therapy, autologous transgenic cell culture techniques for skin regeneration are usually applied to congenital or genetic diseases (Hirsch *et al*., 2017). In fact, the long-term effects associated with the use of gene therapy must be carefully evaluated, the use of polymeric scaffolds in the cutaneous injuries remains a safe and practical approach, for conditions acquired during lifetime. The bioengineering scaffolds should serve as a platform for cellular adhesion, and differentiation, as well as guide the development of new functional tissues. Mostly treatment strategies for skin wounds aim to replace lost tissues rather than support intrinsic self-healing mechanisms. Advances in nanotechnology and biomedical sciences are continuously improving techniques and procedures for skin regeneration and repair.

Histological studies are in progress to further investigate the role of PA-6 and PA-6/SOMA in all phases of the wound healing process. It is possible that these biomaterials find application as synthetic matrices for cell proliferation in deep, partial and full thickness skin injuries. A disadvantage of currently available dermal dressings for wound healing is the poor integration with host tissue. Biosynthetic skin dressings are available to provide temporary or permanent coverage, with the advantages of availability and low risk of infection or immunologic issues. It is difficult to extrapolate the results of animal studies to the case of actual human exposure due to the difference in skin tension and all animal experiments being conducted in a sterile environment (Chen *et al*., 2016). Finally, it is an attempt to suggest that strict *in vivo* animal modeling, including degradation performance and toxicity studies, should be investigated in future on this class of synthetic polymers to evaluatetheir suitability for human use.

4. Conclusions

The results indicated that the polyamide-based biomaterials have outstanding biocompatibility and suitable properties to be applied as a dressing to active carrier biomolecules and guide the development of new functional tissues. The nanofibrous scaffolds showed a dimensional homology to natural ECM components and also promoted the attachment of 3T3 fibroblast and VERO cells, besides incorporating noncovalent PDGF-BB growth factors. Mechanically, the nanomembranes were able to withstand the sterilization process and to conform adequately to the wound surface. The chemical modification of PA-6 chains with a fatty acid derivative led to an increase of surface free energy, which favored cell adhesiveness, collagen formation, and ECM secretion. No side effects were observed in a macroscopic in vivo

evaluation of the wound microenvironment. Although the nanomembranes have not accelerated the wound closure of the animals during the 14 days follow-up, their potential of modulating other healing parameters at a cellular level cannot be excluded. Compared to currently available dermal dressings for skin regeneration, these materials have the added advantages of being ultra-thin, more easily handled and better integrated to host-tissue.

5. Conflict of interest

The authors declare that they have no conflict of interest.

6. Acknowledgements

The authors thank “Mantova Industria de tubos flexíveis” for donating the polyamide and CAPES for the scholarship to Fernanda Dias and Lucas Dall Agnol. This work was supported by CNPq − National Council for Scientific and Technological Development, Brazil (Grants 308241/2015-0). The authors also thank the Brazilian Synchrotron Light Laboratory (LNLS) for the use of their scientific installations (SAXS1 beamline).

7. Authorship Contributions

F.T.G.D., N.F.N. and, O.B. designed the experiments, analyzed the data and wrote the manuscript; A.R.I. contributed in *in vivo* experiments; F.C.M. supported and produced membranes used; L.D. assisted insurface energy characterization; D.R.M. and J.C.C. provided cell culture facilities and contributed in *in vitro* experiments; A.F., J.C.C. and R.M.D.S made a critical review of the manuscript.

8. References

Abdal-hay, A., Khalil, K.A., Al-Jassir, F.F., *et al*. (2017). Biocompatibility properties of polyamide6/PCL blends composite textile scaffold using EA.hy926human endothelial cells. Biomedical Materials, 12, 1-12.*doi:*10.1088/1748-605X/aa6306

Abdal-hay, A., Tijing, L.D.& Lim, J.K. (2013). Characterization of the surface biocompatibility of an electrospun nylon 6/CaP nanofiber scaffold using osteoblastos.Chemical Engineering Journal, 215-216, 57-64.*doi:*0.1016/j.cej.2012.10.046

Andrae, J., Gallini, R. & Betsholtz, C.(2008). Role of platelet-derived growth factors in physiology and medicine. Genes & Development, 22, 1276–1312.*doi:*10.1101/gad.1653708

Aydin, R.S.T., Hazer, B., Acar, M., *et al.*(2013). Osteogenic activities of polymeric soybean oil-g-polystyrene membranes. Polymer Bulletin, 70, 2065–2082.*doi:*10.1007/s00289-013-0976-2

Cai, E.Z., Teo, E.Y., Jing, L., *et al*. (2014). Bio-Conjugated Polycaprolactone Membranes: A Novel Wound Dressing. Archives of Plastic Surgery, 41, 638-646.*doi:*10.5999/aps.2014.41.6.638

Chen, H., Peng, Y., Wu, S., *et al*. (2016). Electrospun 3D Fibrous Scaffolds for Chronic Wound Repair. Materials, 9, 272-283.*doi:*10.3390/ma9040272

Ernzen, J.R., Bondan, F., Luvison, C., *et al*. (2016). Structure and properties relationship of melt reacted polyamide 6/malenized soybean oil. Journal of Applied Polymer Science, 133,1-10.*doi:*10.1002/app.43050

Garcia-Orue, I., Gainza, G., Gutierrez, F.B., *et al*. (2017). Novel nanofibrous dressings containing rhEGF and Aloe vera for wound healing applications. International Journal of Pharmaceutics, 523, 556-566. *doi:*10.1016/j.ijpharm.2016.11.006

Gazzano, M., Gualandi, C., Zucchelli, A., *et al*. (2015). Structure-morphology correlation in electrospun fibers of semicrystalline polymers by simultaneous synchrotron SAXS-WAXD. Polymer, 63, 154-163.*doi:*10.1016/j.polymer.2015.03.002

Grady, B.P. Simple SAXS and WAXS Software written in Excel. http://coecs.ou.edu/Brian.P.Grady/saxssoftware.html

Hirsch, T., Rothoeft, T., Teig, N., *et al.*(2017). Regeneration of the entire human epidermis using transgenic stem cells. Nature.*doi:*10.1038/nature24487

ISO 10993-5 S. (2009). Biological evaluation of medical devices - Part 5: Tests for *in vitro* cytotoxicity. Third edition 2009-06-01 ed2009. 42 p.

Janis, J.E. & Harrison, B. (2014). Wound Healing: Part I. Basic Science. Plastic and Reconstructive Surgery, 133, 199-207.*doi:*10.1097/PRS.0000000000002773

Li, X., Li, Y., Zuo, Y., *et al*. (2015). Osteogenesis and chondrogenesis of biomimetic integrated porous PVA/gel/V-n-HA/pa6 scaffolds and BMSCs construct in repair of articular osteochondral defect.. Journal of Biomedical Materials Research Part A, 103, 3226-3236.*doi:*10.1002/jbm.a.35452

Liu, M., Duan, X-P., Li, Y-M., *et al*. (2017). Electrospun nanofibers for wound healing. Materials Science and Engineering C, 76, 1413-1423. *doi:*10.1016/j.msec.2017.03.034

Lukyanova, L., Franceschi-Messant, S., Vicendo, P., *et al*. (2010). Preparation and evaluation of microporous organogel scaffolds for cell viability and proliferation. Colloids and Surfaces B: Biointerfaces, 79, 105–112.*doi:*10.1016/j.colsurfb.2010.03.044

Mammadov, R., Mammadov, B., Guler, M.O., *et al.*(2012). Growth Factor Binding on Heparin Mimetic Peptide Nanofibers Biomacromolecules, 13, 3311−3319. *doi:*10.1021/bm3010897

Marqués, M.S., Regaño, C., Nyugena, J.,*et al*. (2000). Hydrolytic and fungal degradation of polyamides derived from tartaric acid and hexamethylenediamine. Polymer, 41, 2765-2772.*doi:*10.1016/S0032-3861(99)00422-X

Masrouha, K.Z., El-Bitar, Y., Najjar, M., *et al*. (2016). Epithelialization Over a Scaffold of AntibioticImpregnated PMMA Beads: A Salvage Technique for Open Tibial Fractures with Bone and Soft Tissue Loss When all Else Fails. Archives of Bone and Joint Surgery, 4, 259-263.*doi*:10.22038/abjs.2016.6850

Mensik, I., Lamme, E.N., Riesle, J., *et al*. (2002). Effectiveness and safety of the PEGT/PBT copolymer scaffold as dermal substitute in scar reconstruction wounds (feasibility trial). Cell and Tissue Banking, 3, 245–253.*doi:*10.1023/A:1024674325253

Miao, S., Sun, L., Wang, P., *et al*. (2012). Soybean oil-based polyurethane networks as candidate biomaterials: Synthesis and biocompatibility. European Journal of Lipid Science and Technology, 114, 1165-1174.*doi:*10.1002/ejlt.201200050

White, R. & Morris, C. (2009). Mepitel: a non-adherent wound dressing with Safetac technology. British Journal of Nursing, 18, 58-64.*doi:*10.12968/bjon.2009.18.1.93582

Nur-E-Kamal, A., Ahmed, I., Kamal, J., *et al*. (2008). Covalently attached FGF-2 to three-dimensional polyamide nanofibrillar surfaces demonstrates enhanced biological stability and

activity. Molecular and Cellular Biochemistry, 309, 157-166.*doi:*10.1007/s11010-007-9654-8

Pal, P., Dadhich, P., Srivas, P.K., *et al*. (2017). Bilayered nanofibrous 3D hierarchy as skin rudiment by emulsion electrospinning for burn wound management. Biomaterials Science, 9, 1-31. *doi:*10.1039/C7BM00174F

Park, K., Ju, Y.M., Son, J.S., *et al*. (2007). Surface modification of biodegradable electrospun nanofiber scaffolds and their interaction with fibroblastos. Journal of Biomaterials Science (Polymer Edition), 18, 369-382. *doi:*10.1163/156856207780424997

Reigstad, L.J., Sande, H.M., Fluge, O.,*et al.*(2003). Platelet-derived Growth Factor (PDGF)-C, a PDGF Family Member with a Vascular Endothelial Growth Factor-like Structure. The Journal of Biological Chemistry, 278, 17114-17120.*doi:*10.1074/jbc.M301728200

Richard-Lacroix, M. & Pellerin, C. (2013). Molecular Orientation in Electrospun Fibers: From Mats to Single Fibers. Macromolecules, 46, 9473−9493.*doi:*10.1021/ma401681m

Rieger, K.A., Birch, N.P. & Schiffman, J.D. (2013). Designing electrospun nanofiber mats to promote wound healing – a review. Journal of Materials Chemistry B, 1, 4531-4541.*doi:*10.1039/C3TB20795A

Santin, M. & Ambrosio, L. (2008). Soybean-based biomaterials: preparation, properties and tissue regeneration potential. Expert Review of Medical Devices, 5, 349-358. *doi:*10.1586/17434440.5.3.349

Schindler, M., Ahmed, I., Kamal, J., *et al*. (2005). A synthetic nanofibrillar matrix promotes in vivo-like organization and morphogenesis for cells in culture. Biomaterials, 26, 5624-5631.*doi:*10.1016/j.biomaterials.2005.02.014

Smiell, J.M., Wieman, T.J., Steed, D.L., *et al.*(1999). Efficacy and safety of becaplermin (recombinant human platelet-derived growth factor-BB) in patients with nonhealing, lower extremity diabetic ulcers: A combined analysis of four randomized studies. Wound Repair and Regeneration, 7, 335–346.*doi:*10.1046/j.1524-475X.1999.00335.x

Stachewicz, U. & Barber, A.H. (2011). Enhanced Wetting Behavior at Electrospun Polyamide Nanofiber Surfaces. Langmuir, 27, 3024-3029.*doi:*10.1021/la1046645

Stephens, J.S., Chase, D.B. & Rabolt, J.F.(2004). Effect of the Electrospinning Process on Polymer Crystallization Chain Conformation in Nylon-6 and Nylon-12. Macromolecules, 37, 877-881.*doi:*10.1021/ma0351569

Tsou, S-Y., Lin, H-S. and Wang, C. (2011). Studies on the electrospun Nylon 6 nanofibers from polyelectrolyte solutions: 1. Effects of solution concentration and temperature. Polymer, 52, 3127-3136. *doi:*10.1016/j.polymer.2011.05.010

Uhl, E., Rösken, F., Sirsjö, A., *et al*. (2003). Influence of platelet-derived growth factor on microcirculation during normal and impaired wound healing. Wound Repair and Regeneration, 11, 361–367. *doi:*10.1046/j.1524-475X.2003.11508.x

Unnithan, A.R., Barakat, N.A.M., Pichiah, P.B.T., *et al*. (2012). Wound-dressing materials with antibacterial activity from electrospun polyurethane–dextran nanofiber mats containing ciprofloxacin HCl. Carbohydrate Polymers, 90, 1786-1793.*doi:*10.1016/j.carbpol.2012.07.071

Xie,D., Seremwe, M., Edwards, J.G., *et al*. (2014). Distinct effects of different phosphatidylglycerol species on mouse keratinocyte proliferation.PloS One, 9, 1-9.*doi:*10.1371/journal.pone.0107119

Yang, L., Kandel, R.A., Chang, G., *et al*. (2009). Polar surface chemistry of nanofibrous polyurethane scaffold affects annulus fibrosus cell attachment and early matrix accumulation. Journal of Biomedical Materials Research Part A, 91, 1089-1099.*doi:*10.1002/jbm.a.32331

Yang, Y., Xia, T., Chen, F., *et al*. (2012). Electrospun Fibers with Plasmid bFGF Polyplex Loadings Promote Skin Wound Healing in Diabetic Rats. Molecular Pharmaceutics,9, 48-58.*doi:*10.1021/mp200246b

Zajicova, A., Pokorna, K., Lencova, A., *et al*. (2010). Treatment of ocular surface injuries by limbal and mesenchymal stem cells growing on nanofiber scaffolds. Cell Transplant, 19, 1281-1290.*doi:*10.3727/096368910X509040

FIGURE LEGENDS

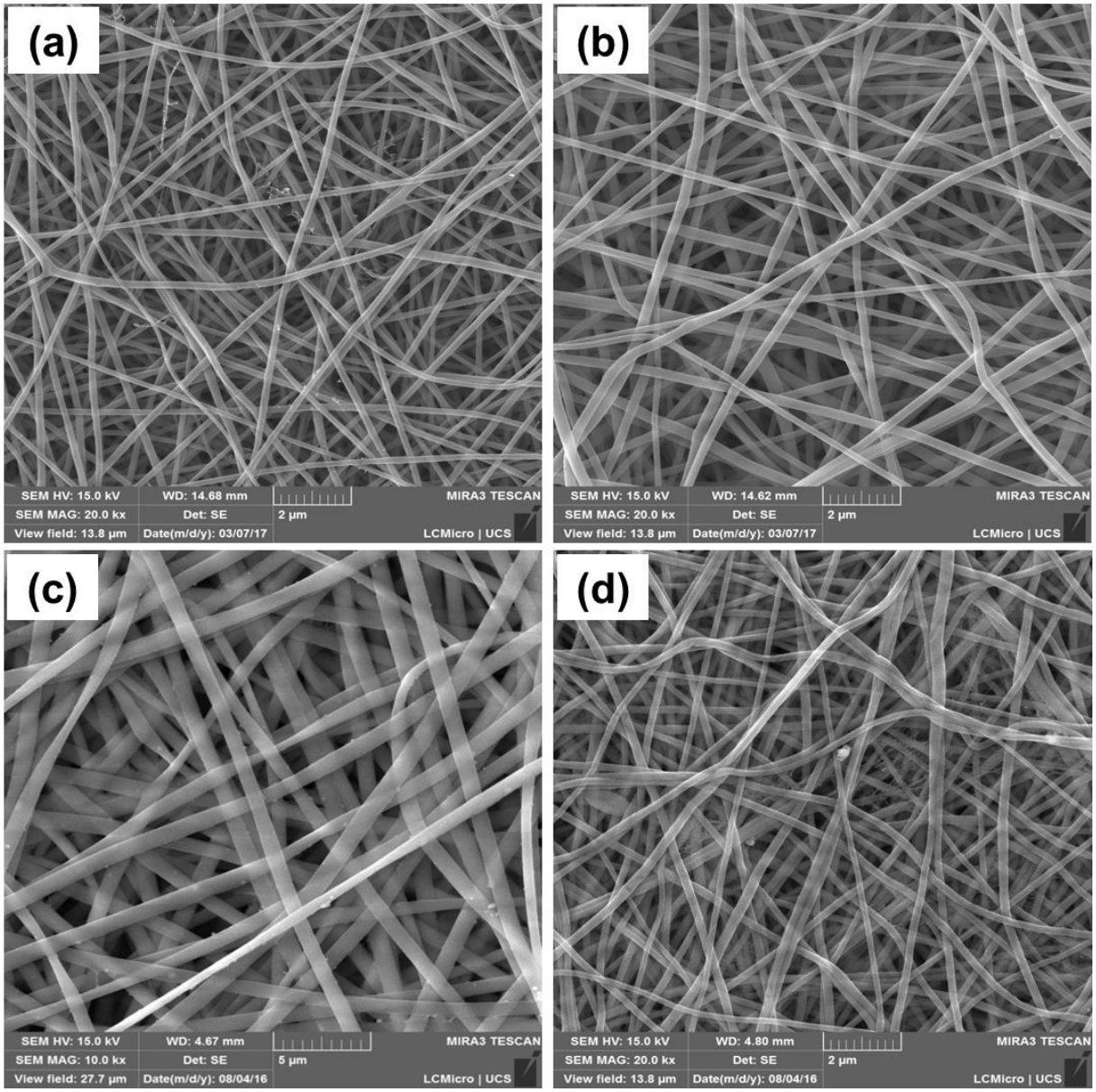

Figure1: Morphological appearance (FEG/SEM) of electrospun materials at 32%wt: (a) commercial PA-6; (b) PA-6/SOMA (95/5); (c) sterilized commercial PA-6 and (d) sterilizedPA-6/SOMA (95/5).

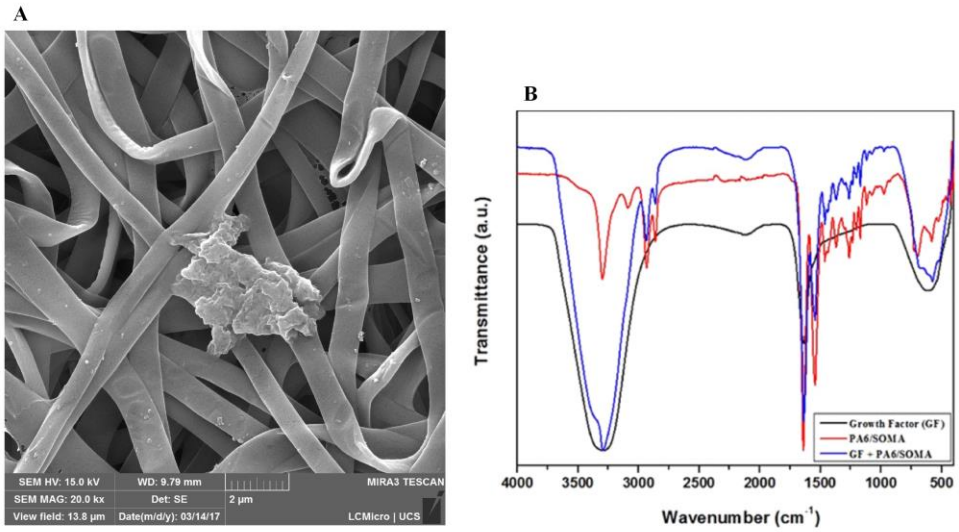

Figure 2: Evidence of PDGF-BB incorporation into PA-6/SOMA nanomembrane by (A) FEG-SEM and (B) FTIR (FEG-SEM magnification 20.0 kx).

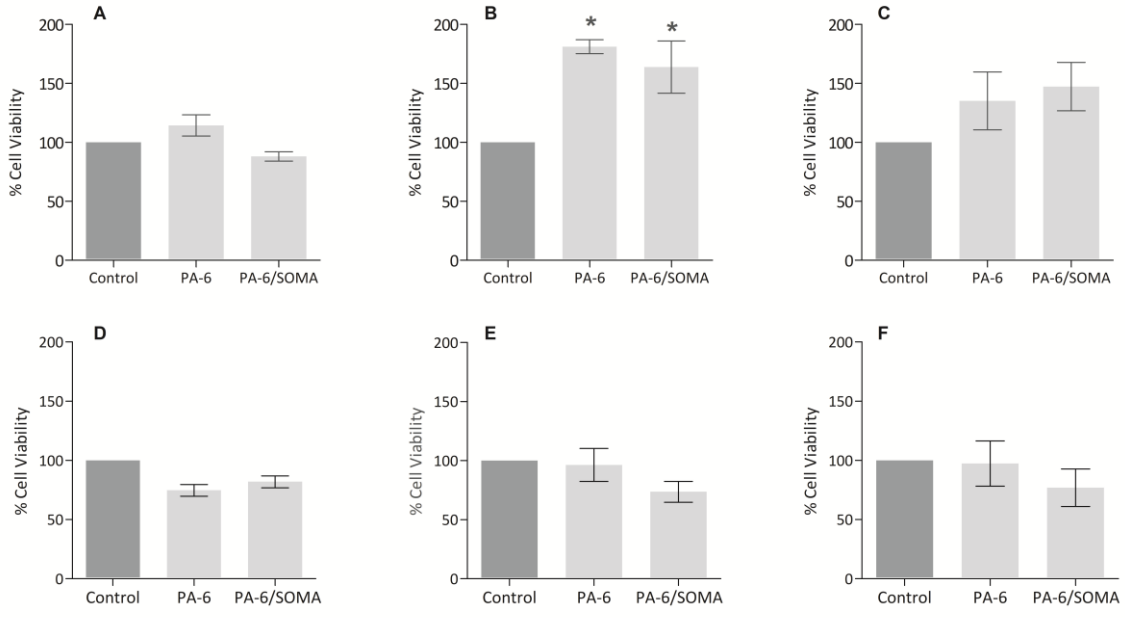

Figure 3: Effect of incubation with PA-6 and PA-6/SOMA nanomembranes on cell viability of 3T3 murine fibroblast cells after (A) 24 h, (B) 48 h and (C) 72 h and VERO cells after (D) 24 h, (E) 48 h and (F) 72 h. The experiments were carried out at least three times in triplicate. Each column represents the mean±SEM. *$p<0.05$ versus control.

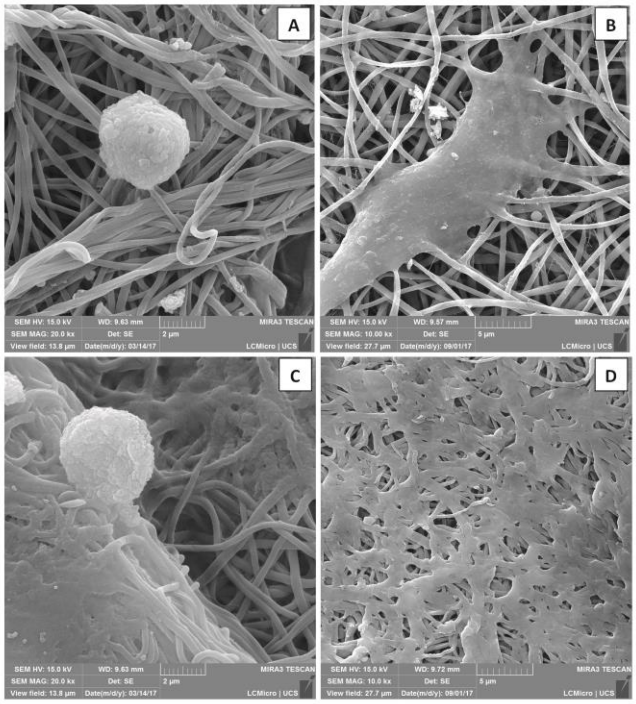

Figure4: Fibroblast 3T3 adhesion in (A) commercial PA-6, 24 h; (B) PA-6/SOMA, 24 h; (C) commercial PA-6, 72 h; (D) PA-6/SOMA, 72 h (FEG-SEM magnification 10.0 kx; 20.0 kx).

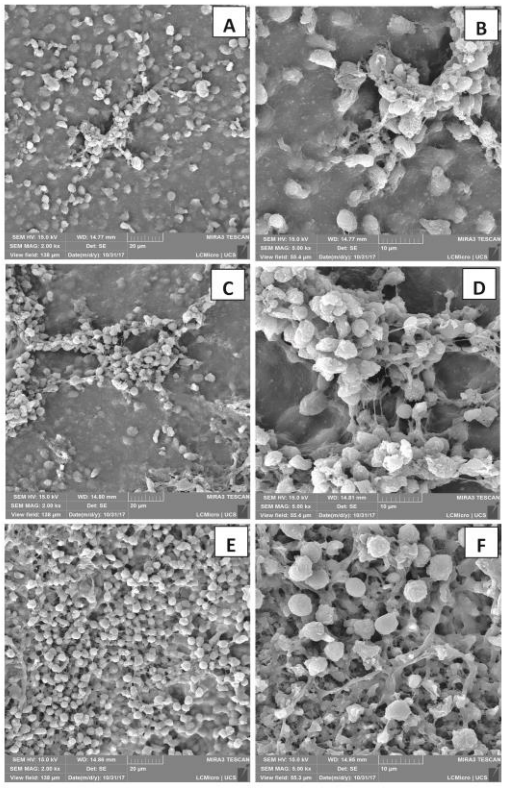

Figure 5: FEG-SEM analysis of (A, B) commercial PA-6; (C, D) PA-6/SOMA and (E, F) PA-6/SOMA loaded with PDGF-BB nanomembrane behavior in direct contact with the wound 72 hours after application (FEG-SEM magnification 2.0 kx; 5.0 kx).

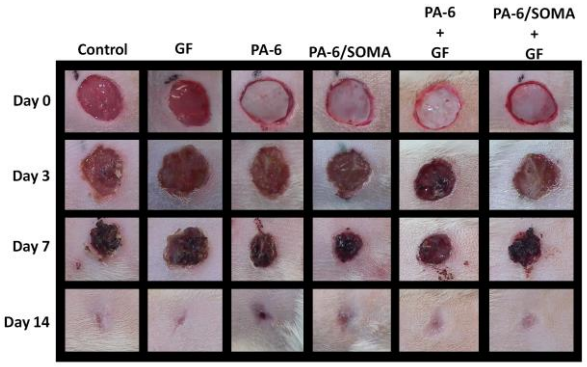

Figure 6: Representative images of wounds over the course of the healing process on days 0, 3, 7 and 14. Scale Bar = 10 mm.

SUPPLEMENTARY FILES

Table S1: Optimization of PA-6 and PA-6/SOMA electrospinning process

Polymer	Solvent	Concentration	Voltage	Distance	Feeding rate	Humidity	System behavior
PA-6	Formic acid	**20%wt**	20 - 30 kV	15 cm	1.0 mL/h	58%	Continuous dripping
			20 - 30 kV	10 cm	1.0 mL/h		Continuous dripping
			25 kV	7 cm	0.5 mL/h		Continuous dripping
			25 kV	6 cm	0.5 mL/h		Fiber segments
PA-6	Formic acid	**22%wt**	20 - 30 kV	8 cm	1.0 mL/h	54%	Continuous dripping
PA-6	Formic acid	**28%wt**	20 - 23 kV	17,5 cm	0.1 mL/h	52%	Dripping every 20 s
			20 - 23 kV	17,5 cm	0.15 mL/h		Dripping
			11 – 23 kV	19 cm	0.1 mL/h		No dripping and no fiber formation
			18 kV	15 cm	0.2 mL/h		Fiber segment + drop
PA-6/SOMA	Formic acid	**30% wt**	18 – 25 kV	10 cm	1.0 mL/h	52%	Continuous dripping
			18 – 25 kV	10 cm	2.0 mL/h		Continuous dripping
			18 – 25 kV	10 cm	3.0 mL/h		Continuous dripping
			20 - 25 kV	13 cm	0.5 mL/h		Continuous dripping
			20 - 25 kV	13 cm	1.0 mL/h		Continuous dripping

			20 - 25 kV	13 cm	2.0 mL/h		Continuous dripping
			20 - 25 kV	15 cm	0.5 mL/h		Continuous dripping
			20 - 25 kV	15 cm	1.0 mL/h		Continuous dripping
			20 - 25 kV	15 cm	2.0 mL/h		Continuous dripping
			10 - 15 kV	15 cm	0.1- 0.5 mL/h		Dripping at longer intervals
			8 - 20 kV	18 cm	0.1 mL/h		Fiber segment + drop
			8 - 20 kV	18 cm	0.3 mL/h		Fiber segment + drop
			20 – 24 kV	20 cm	0.2 mL/h		Dripping at longer intervals
			24 kV	20 cm	0.1 mL/h		Fibers + isolated drops
PA-6/SOMA	Formic acid	**32%wt**	24 kV	20 cm	0.1 mL/h	57%	Formation of a whitish thin film on the collector
			24 kV	20 cm	0.2 mL/h		Formation of a whitish thin film on the collector
			24 kV	20 cm	0.3 mL/h		Dripping at longer intervals
			24 kV	20 cm	0.5 mL/h		Dripping at longer intervals
			25 kV	15 cm	0.1 mL/h		Fibers
PA-6			25 kV	15 cm	0.1 mL/h		Fibers
PA-6/SOMA	Formic acid	**35%wt**	25 kV	15 cm	0.1 mL/h	57%	Fibers
PA-6			25 kV	12 cm	0.1 mL/h		Fibers

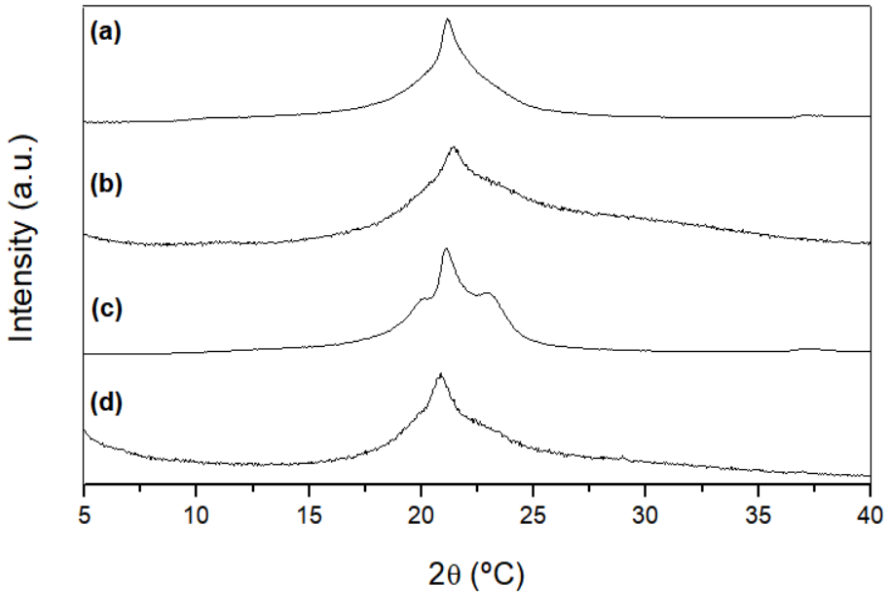

Fig. S1: WAXD results for solid commercial PA-6 (a), commercial PA-6 electrospun mat (b), solid PA-6/SOMA (c) and PA-6/SOMA electrospun mat (d).

Table S2: Relative fractional crystallinity and amount of γ-form polyamide crystals from WAXD pattern deconvolution

SAMPLES	**Amorphous Peak (º)**	**1st Peak (º)**	**2nd Peak (º)**	**3rd Peak (º)**	**4th peak (º)**	**Amorphous Fraction (%)**	**Crystalline Fraction (%)**	**Gamma (%)**
Solid commercial PA-6	19.29	21.27	21.33	21.47	21.14	30.30	69.70	0.56
Electrospun comercial PA-6	27.78	20.50	21.14	21.41	22.12	59.21	40.79	0.16
Solid PA-6/SOMA	19.90	20.62	23.23	21.7	21.14	31.41	68.59	0.69
Electrospun PA-6/SOMA	24.88	21.14	19.95	20.84	21.46	48.65	51.35	0.16

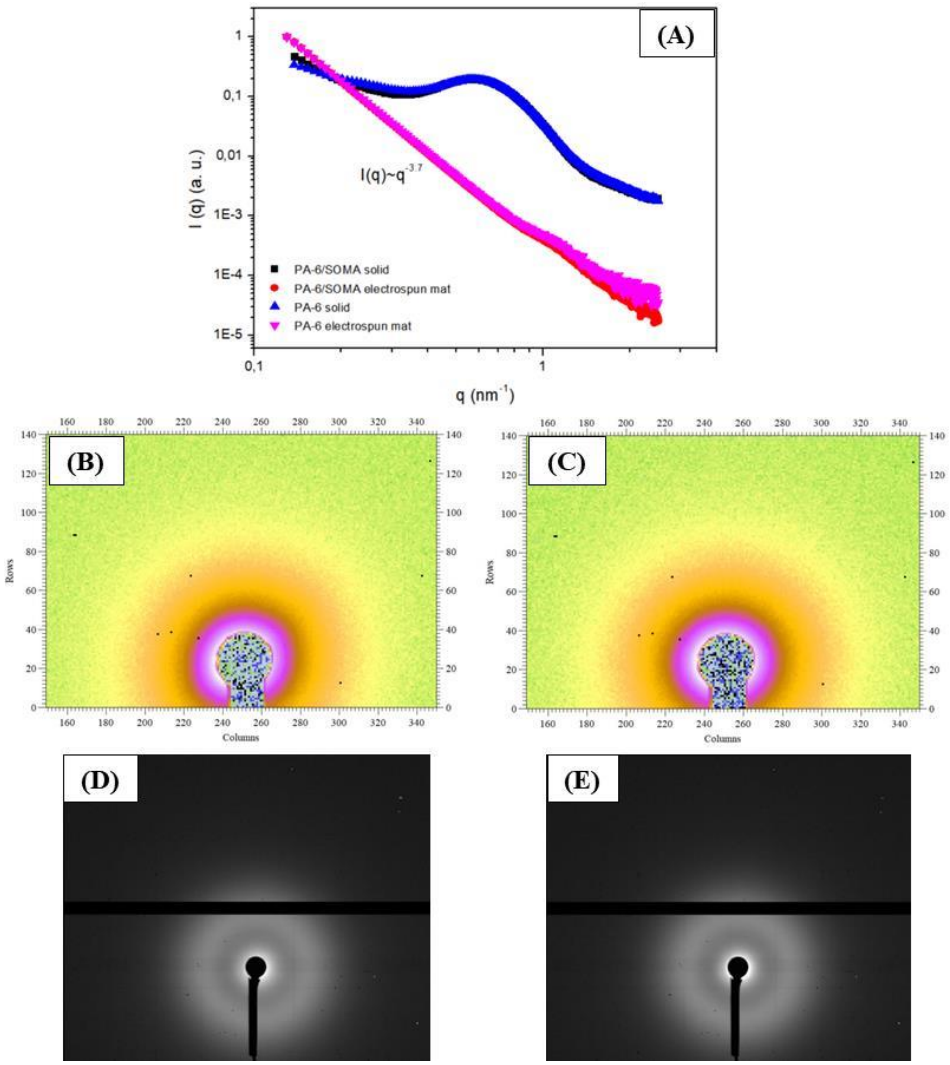

Fig. S2: SAXS curves for the materials (A) and 2D patterns for electrospun PA-6 (B), electrospun PA-6/SOMA (C), solid PA-6 (D) and solid PA-6/SOMA (E).

Table S3: Contact angles (θ, ºC) and surface free energy (γ_S) of the solid surfaces, including dispersive (γ_S^D) and polar (γ_S^P) contributions [10]

Solid surfaces	**Contact Angle (θ, ºC)**					**Surface free energy (mN/m)**			**R^2**
	Water	Glycerin	Dimethyl sulfoxide	n-Hexadecane	BSA	γ_S	γ_S^D	γ_S^P	
PA-6	82.6 ± 0.8	82.5 ± 1.2	44.9 ± 0.6	11.2 ± 0.6	94.3 ± 0.4	47.5	37.2	10.3	0.9847
PA-6/SOMA	81.7 ± 0.9	75.9 ± 0.7	38.3 ± 0.7	7.9 ± 1.1	74.3 ± 0.2	55.9	42.2	13.7	0.9923

[10] U. Stachewicz, A.H. Barber, Enhanced Wetting Behavior at Electrospun Polyamide Nanofiber Surfaces, Langmuir 27 (2011) 3024–3029

Dear Mr. Ricardo Ingracio,

You have been listed as a Co-Author of the following submission:

Journal: Materials Science & Engineering C

Title: Polymeric electrospun mats as cutaneous topical dressing for chronic wounds

Corresponding Author: FERNANDA TRINDADE

Co-Authors: Anderson Ricardo Ingracio, Natália Fontana Nicoletti, Felipe Menezes, Lucas Dall Agnol, Daniel Marinowic, Rosane Soares, Jaderson da Costa, Asdrubal Falavigna, Otávio Bianchi

FERNANDA TRINDADE submitted this manuscript via Elsevier's online submission system, EVISE®. If you are not already registered in EVISE®, please take a moment to set up an author account by navigating to http://www.evise.com/evise/faces/pages/navigation/NavController.jspx?JRNL_ACR=MSEC

If you already have an ORCID, we invite you to link it to this submission. If the submission is accepted, your ORCID will be transferred to ScienceDirect and CrossRef and published with the manuscript.

To link an existing ORCID to this submission, or sign up for an ORCID if you do not already have one, please click the following link: Link ORCID

What is ORCID?

ORCID is an open, non-profit, community-based effort to create and maintain a registry of unique researcher identifiers and a transparent method of linking research activities and outputs to these identifiers.

More information on ORCID can be found on the ORCID website, http://www.ORCID.org, or on our ORCID help page:
http://help.elsevier.com/app/answers/detail/a_id/2210/p/7923

If you did not co-author this submission, please contact the Corresponding Author directly at ftgdias@ucs.br.

Thank you,
Materials Science & Engineering C

This message was sent automatically. Please do not reply